Earth Surf. Dynam. Discuss., doi:10.5194/esurf-2017-28, 2017
Manuscript under review for journal Earth Surf. Dynam.
Discussion started: 8 May 2017

Developing and evaluating a theory for the lateral erosion of bedrock channels for use in landscape evolution models

Abigail L. Langston[1] and Gregory E. Tucker[2,3]

[1]Department of Geography, Kansas State University, Manhattan, USA
[2]Cooperative Institute for Research in Environmental Sciences (CIRES), University of Colorado, Boulder, USA
[3]Department of Geological Sciences, University of Colorado, Boulder, USA

Correspondence to: A.L. Langston (alangston@ksu.edu)

Abstract. Understanding how a bedrock river erodes its banks laterally is a frontier in geomorphology. Theory for the vertical incision of bedrock channels is widely implemented in the current generation of landscape evolution models. However, in general existing models do not seek to implement the lateral migration of bedrock channel walls. This is problematic, as modeling geomorphic processes such as terrace formation and hillslope-channel coupling depends on accurate simulation of valley widening. We have developed and implemented a theory for the lateral migration of bedrock channel walls in a catchment-scale landscape evolution model. Two model formulations are presented, one representing the slow process of widening a bedrock canyon, the other representing undercutting, slumping, and rapid downstream sediment transport that occurs in softer bedrock. Model experiments were run with a range of values for bedrock erodibility and tendency towards transport- or detachment-limited behavior and varying magnitudes of sediment flux and water discharge in order to determine the role each plays in the development of wide bedrock valleys. Results show that this simple, physics-based theory for the lateral erosion of bedrock channels produces bedrock valleys that are many times wider than the grid discretization scale. This theory for the lateral erosion of bedrock channel walls and the numerical implementation of the theory in a catchment-scale landscape evolution model is a significant first step towards understanding the factors that control the rates and spatial extent of wide bedrock valleys.

1 Introduction and Motivation

Understanding the processes that control the lateral migration of bedrock rivers is fundamental for understanding the genesis of landscapes in which valley width is many times the channel width. Strath terraces are a clear indication of a landscape that has experienced an interval where lateral erosion has outpaced vertical incision (Hancock and Anderson, 2002). Broad strath terraces that are many times wider than the channels that carved them are found in mountainous and hilly landscapes throughout the world (e.g. Chadwick et al., 1997; Lavé and Avouac, 2001; Dühnforth et al., 2012) and provide clues about the nature of their evolution.

Changes in climate that drive changes in sediment flux, changes in discharge magnitude, and/or changes in discharge frequency have been cited as causes of periods of lateral erosion in bedrock rivers. The frequency of intense rain is correlated with higher channel sinuosity and lateral erosion rates on regional scales (Stark et al., 2010). Several studies demonstrate that significant lateral erosion in rapidly incising rivers is accomplished by large flood events (Hartshorn et al., 2002; Barbour et al., 2009), resulting from armoring of the bed during extreme flood events (Turowski et al., 2008) and exposure of the bedrock walls to sediment and flow (Beer et al., 2017). Sediment cover on the bed that suppresses vertical incision and allows lateral erosion to continue unimpeded is a critical element for the development of wide bedrock valleys, as determined from modeling, field, and experimental studies (Hancock and Anderson, 2002; Brocard and Van der Beek, 2006; Johnson and Whipple, 2010). Lateral erosion that outpaces vertical incision and creates wide bedrock valleys is linked to weak underlying lithology, such as shale (Montgomery, 2004; Snyder and Kammer, 2008; Schanz and Montgomery, 2016). The relationships among river sediment flux, discharge, lithology, and rates of lateral bedrock erosion are not well defined. Because we do not sufficiently understand the processes of lateral erosion, landscape evolution models lack a physical mechanism for allowing channels to migrate laterally and widen bedrock valleys, in addition to incising bedrock valleys.

Theory for the vertical incision of bedrock channels has advanced considerably since the first physics-based bedrock incision models were presented in the early 1990's. For example, bedrock incision models now include theories for adjustment of channel width (Wobus et al., 2006; Turowski et al., 2009; Yanites and Tucker, 2010), the role of sediment size and bed cover (Whipple and Tucker, 2002; Sklar and Dietrich, 2004; Yanites et al., 2011), and thresholds for incision (Tucker and Bras, 2000; Snyder et al., 2003b). Rivers respond to changing boundary conditions by adjusting both slope and channel width (Lavé and Avouac, 2001; Duvall et al., 2004; Snyder and Kammer, 2008) and landscape evolution models must be able capture both of these responses if we are to fully describe the behavior and function of landscapes. Research on bedrock channel width gives important insights into the larger scale problem of bedrock valley widening. In particular, the effects of sediment cover on the bed play an important role in the evolution of channel cross-sectional shape because sediment cover on the bed can slow or halt vertical incision (Sklar and Dietrich, 2004; Turowski et al., 2007), while allowing lateral erosion to continue. Models of channel cross-sectional evolution predict that increasing sediment supply to a steady-state stream results in a wider, steeper channel for a given rate of base level fall (Yanites and Tucker, 2010).

Theories that account for adjustment to channel width, sediment size and cover, and incision thresholds are assimilated in the current generation of landscape evolution models (Tucker and Hancock, 2010). However, existing models rarely treat lateral erosion of bedrock channel walls and the consequential migration of the channel, in no small part because of the lack of a rigorous understanding of the processes that control lateral erosion of bedrock channel walls. If this theoretical hurdle can be cleared, an algorithm for lateral erosion must be applied within a framework of models that currently only erode and deposit vertically. To our knowledge, this study is the first attempt at incorporating a generalized physics-based algorithm for lateral bedrock erosion and channel migration on a drainage basin scale to a two-dimensional landscape evolution model.

Lateral migration of bedrock channel walls has only been implemented into landscape evolution models in a few specialized studies (Lancaster, 1998; Hancock and Anderson, 2002; Clevis et al., 2006a; Finnegan and Dietrich, 2011; Limaye and Lamb, 2013). Hancock and Anderson (2002) reproduce valley widening using a 1-D stream power model for vertical incision and assume that valley widening rates depend on stream power. They note that the width of the valley floor is related to the duration of steady state in the river, as theorized by Suzuki (1982). This model is based on the key observation that lateral erosion exceeds vertical incision when the channel is carrying the maximum sediment load dictated by the transport capacity.

Earth Surf. Dynam. Discuss., doi:10.5194/esurf-2017-28, 2017
Manuscript under review for journal Earth Surf. Dynam.
Discussion started: 8 May 2017

By varying sediment supply to the channel, their model predicts the development of a series of strath terraces. Strath terrace sequences have also been produced by coupling a meandering model with a river incision model (Finnegan and Dietrich, 2011). Lateral migration of a meandering channel has been implemented in several landscape evolution models. Clevis et al. (2006a) modeled meandering channels in a valley section using a 2-D landscape evolution model and an adaptive grid approach. A vector-based approach to modeling lateral migration of meandering streams in heterogeneous bed material has been used to reproduce a range of bedrock valley forms (Limaye and Lamb, 2014), but this model is primarily a channel-scale model. While each of these studies model lateral migration of bedrock channel banks, they all operate with a meandering model that is not applicable to lateral migration in low-sinuosity channels or in a generalized landscape evolution model.

Until now, landscape evolution models have lacked a generic mechanism for allowing channels to migrate laterally and widen bedrock valleys, as well as incise bedrock valleys. While advances in controls on bedrock valley width have been made using meandering models, the representation of a sinuous channel doesn't describe all rivers, and often such models are constructed on a channel scale rather than on a drainage basin scale. In this study, we develop a theory for the lateral migration of bedrock channel walls and implement this theory in a 2-D landscape evolution model for the first time. We seek to explore the parameters that exert primary control on the morphology of bedrock valleys and the rate of bedrock valley widening using a series of numerical experiments.

Our objective is to define and explore a theory for lateral erosion that has the following characteristics: simple and sufficiently general in nature to be applicable in landscape evolution models; containing as few parameters as possible; requiring relatively few input variables, such as channel gradient and water discharge plus gross channel planform configuration. The aim of this theory is to model valley widening or narrowing over time scales relevant to drainage basin evolution, and across multiple branches within a drainage network. The theory is not designed to predict the movement of a particular channel segment over a period of a few years, but rather is intended to provide a general basis for understanding when and why valleys tend to narrow or widen during the course of their long-term geomorphic evolution. Theoretical predictions about these trends then serve as quantitative, mechanistically based hypotheses that can be tested by experiment and observations. Through a set of numerical experiments, we seek to answer the following set of questions:

- How does this lateral erosion model compare with purely vertical erosion models?
- How do two alternative formulations, which treat bank material differently, compare to each other?
- What combinations of bedrock erodibility, sediment mobility, water flux, sediment flux, and model type result in wide bedrock valleys?
- What are predictions of the model that could be readily tested through experiment and/or observation?

In the following sections we outline our theory for lateral channel wall migration and explain the two algorithms we have developed to apply this theory to an existing model. We then present the results from our set of numerical experiments and discuss how well the model describes the formation of wide bedrock valleys.

Earth Surf. Dynam. Discuss., doi:10.5194/esurf-2017-28, 2017
Manuscript under review for journal Earth Surf. Dynam.
Discussion started: 8 May 2017

2 Theory

We have deliberately chosen the most simple formulation possible for deposition and erosion, while still capturing the role of sediment. We do this in order to focus on developing the lateral erosion component of our model. Evolution of the height of the landscape, η, through time is described by deposition rate, d, minus erosion rate, e, plus a constant rate of uplift relative to baselevel, U.

$$\frac{\partial \eta}{\partial t} = -e + d + U \tag{1}$$

Deposition rate is assumed to depend on the concentration of sediment (C_s) in active transport and its effective settling velocity, ν_s. Sediment concentration is expressed as the ratio of volumetric sediment flux, Q_s, to water discharge, Q:

$$C_s = \frac{Q_s}{Q} \tag{2}$$

We treat water discharge as the product of runoff rate and drainage area, such that $Q = RA$. Deposition rate is therefore given by:

$$d = \frac{\nu_s d_* Q_s}{RA} \tag{3}$$

where d_* is a dimensionless number describing the vertical distribution of sediment in the water column, which is equal to 1 if sediment is equally distributed through the flow (Davy and Lague, 2009). ν_s, d_*, and R are lumped into a single dimensionless parameter, α, that represents the potential for deposition.

$$\alpha = \frac{\nu_s d_*}{R} \tag{4}$$

A larger α implies more rapid deposition (all else being equal), either because settling velocity, ν_s, is high and sediment is quickly lost from the flow, or because runoff rate, R is low and there is little water in the channels to dilute the sediment. A smaller α represents slower settling velocity, or more intuitively, greater runoff. α can be thought of as a sediment mobility number: when $\alpha < 1$, sediment is easily transported and the model tends towards detachment-limited behavior; when $\alpha > 1$, sediment is less mobile and the model tends towards transport-limited behavior.

2.1 Vertical erosion theory

Vertical erosion rate is derived from the rate of energy dissipation on the channel bed, which is given by

$$\omega_v = \rho g \frac{Q}{W} S \tag{5}$$

Earth Surf. Dynam. Discuss., doi:10.5194/esurf-2017-28, 2017
Manuscript under review for journal Earth Surf. Dynam.
Discussion started: 8 May 2017

where ρ is the density of water, g is gravitational acceleration, Q is water discharge, W is channel width, and S is channel slope. The rate of vertical erosion scales as

$$E_v = K_v^{'} \frac{\omega_v}{C_e} \tag{6}$$

where $K_v^{'}$ is a dimensionless vertical erosion coefficient and C_e is cohesion of bed and bank material. We use bulk cohesion simply as a convenient reference scale for rock resistance to erosion. This choice allows us to express erosion rate as a function of the hydraulic power applied (ω_v), a commonly used measure of material strength (C_e), and a dimensionless efficiency factor ($K_v^{'}$). Substituting RA for Q and $k_w Q^{1/2}$ for W in equation 5, and combining equations 5 and 6 gives:

$$E_v = \frac{K_v^{'} \rho g R^{1/2}}{k_w C_e} A^{1/2} S \tag{7a}$$

$$E_v = K_v A^{1/2} S \tag{7b}$$

where k_w is a width coefficient. Lumping several parameters gives K_v, a dimensional vertical erosion coefficient (with units of years^{-1}), which consists of known or measurable quantities, and one unknown dimensionless parameter, $K_v^{'}$.

2.2 Lateral erosion theory

Lateral erosion requires hydraulic energy expenditure to damage the bank material and/or dislodge previously weathered particles (Suzuki, 1982; Lancaster, 1998; Hancock and Anderson, 2002). We hypothesize that the lateral erosion rate is proportional to the rate of energy dissipation per unit area of the channel wall created by centripetal acceleration around a bend. Erosion of the channel wall is the result of the force of water acting on the channel wall. We know from basic physics that the force of water acting on the wall is equal to the force of the wall acting on the water, which is equal to centripetal force. Centripetal force is $F_c = m\frac{v^2}{r_c}$, where m is mass, v is velocity, and r_c is radius of curvature. The centripetal force of a unit of water can be found by replacing m with ρLHW, where ρ is the density of water, and L, H, and W are unit length, water depth, and channel width, respectively. Centripetal force of water flowing around a bend can be expressed in terms of centripetal shear stress, which is analogous to bed shear stress, by dividing both sides by HL giving:

$$\sigma_c = \frac{\rho W v^2}{r_c} \tag{8}$$

Centripetal shear stress can be turned into a rate of energy expenditure by multiplying by fluid velocity, giving:

$$\omega_c = \frac{\rho W v^3}{r_c} \tag{9}$$

Earth Surf. Dynam. Discuss., doi:10.5194/esurf-2017-28, 2017
Manuscript under review for journal Earth Surf. Dynam.
Discussion started: 8 May 2017

To express this in terms of discharge, Q, instead of velocity, we employ the Darcy-Weisbach equation, giving $v^3 = gqS/F$, where q is discharge per unit width and F is a friction factor, which yields

$$\omega_c = \frac{\rho g Q S}{r_c F} \tag{10}$$

Equation 10 describes a quantity that might be termed centripetal unit stream power, as it represents the rate of energy dissipation per unit bank area. The centripetal unit stream power is similar to the more familiar quantity unit stream power, except that channel width is replaced by the radius of curvature multiplied by a friction factor.

We hypothesize that lateral erosion rate scales with energy dissipation rate around a bend according to

$$E_l = K_l^{'} \frac{\omega_c}{C_e} \tag{11}$$

where $K_l^{'}$ is a dimensionless lateral erosion coefficient. Combining equations 10 and 11 gives

$$E_l = \frac{K_l^{'} \rho g R}{C_e F} \frac{AS}{r_c} \tag{12a}$$

$$E_l = K_l \frac{AS}{r_c} \tag{12b}$$

where K_l is a dimensional erosion coefficient for lateral erosion, which is composed of known or measurable quantities, and one unknown dimensionless parameter, $K_l^{'}$. If $K_l^{'}$ is equal to $K_v^{'}$, we find a ratio between K_l and K_v, given by

$$\frac{K_l}{K_v} = \frac{R^{1/2} k_w}{F} \tag{13}$$

which consists of runoff rate, R, bank width coefficient, k_w, and friction factor, F. We can measure or make reasonable estimates of each of these parameters in order to determine what the ratio of lateral to vertical erodibility should be. Runoff rate can vary widely, but a higher runoff intensity will lead to a higher K_l/K_v ratio and more lateral erosion, as suggested by field observations of lateral erosion in bedrock channels (Hartshorn et al., 2002) and correlation of increased sinuosity and storminess of climate (Stark et al., 2010).

A bank width coefficient of 10 m/(m^3/s)$^{1/2}$ is reasonable for a range of natural rivers (Leopold and Maddock, 1953). If k_w is lower, then the channel is more narrow and water is deeper, and more vertical incision should occur. The friction factor, F, is the Darcy-Weisbach friction factor, which can range from 0.01–1.0 for natural rivers (Gilley et al., 1992; Hin et al., 2008). With a lower friction factor (representing smooth channel walls), the lateral erosion ratio would be higher due to less energy being dissipated on the channel walls, leaving more energy available for lateral erosion.

Earth Surf. Dynam. Discuss., doi:10.5194/esurf-2017-28, 2017
Manuscript under review for journal Earth Surf. Dynam.
Discussion started: 8 May 2017

3 Numerical implementation

One challenge in modeling both vertical and lateral erosion in a drainage network lies in the representation of topography. Normally, landscape evolution models use a numerical scheme in which the terrain is represented by a grid of points whose horizontal positions are fixed and whose elevation represents the primary state variable in the model. Such a framework does not lend itself to the motion of near-vertical to vertical interfaces (such as stream banks and cliffs), and for this reason, incorporating lateral stream erosion in a conventional landscape evolution model requires a modification to the basic numerical framework. A vertical rather than horizontal grid (Kirkby, 1999) can be used for near-vertical landforms in isolation, but is inappropriate when one wishes to represent vertical interfaces that are inset within a larger landscape. Grid-node movement combined with adaptive re-gridding (Clevis et al., 2006a, b) provides a possible solution, but is computationally expensive, and particularly difficult to implement when multiple branches of a drainage network may undergo lateral motion. Here, we adopt a simpler approach in which valley walls are viewed as sub-grid-scale features that migrate through the fixed grid. Rather than tracking the position of these vertical interfaces, we instead track the cumulative sediment volume that has been removed from the cell surrounding a given grid node as a result of lateral erosion. When that cumulative loss exceeds a threshold volume, the elevation of the grid node is lowered.

More specifically, at each node in the model, we calculate a vertical incision rate at the primary node and a lateral erosion rate at a neighboring node. The lateral neighbor node for the primary node is chosen on the outside bank of two stream segments that flow into and out of the primary node. The stream segments used to identify the neighboring node over which lateral erosion should occur are the incoming stream segment to the primary node with the greater drainage area and the stream segment that connects the primary node to its downstream neighbor (Figure 1). If the two segments are straight, then a neighboring node of the primary node is chosen at random and lateral erosion occurs at this node until elevation changes at the node. Calculation of radius of curvature along two stream segments in a raster grid with D8 flow routing presents a challenge, as the angle between segments is discretized; the two segments may form a straight line, in which case the angle is equal to 0°, form a 45° angle, or form a 90° angle. In order to reduce the impact of this discretization, we assume that each of these three cases represents a continuum of possible radii of curvature. Cases of two straight segments are treated as if the actual angle between them ranges anywhere between +22.5° to -22.5°. If one takes the average among these possible angles, the resulting radius of curvature is $0.23dx$, where dx is the cell size in the flow direction. Similarly, we assume that a 45° bend represents a continuum of possible angles between the two segments, ranging from 22.5°-63.5°, resulting in a radius of curvature of $0.67dx$. Following the same principle for a 90° bend gives a mean radius of curvature of $1.37dx$.

The volumetric rate of material eroded laterally for each lateral node is calculated by $E_l \times dx \times H$, where H is water depth, given in meters. Water depth at each node is calculated by $H = 0.4Q^{0.35}$ (Andrews, 1984), where Q is given in m^3/s. The volume of sediment eroded laterally per time step is sent downstream along with any material eroded from the primary cell. Volumetric erosion rate is multiplied by the time step duration to get the volume eroded at the lateral nodes, and the cumulative volume eroded from each lateral node is tracked throughout the entire model run.

Earth Surf. Dynam. Discuss., doi:10.5194/esurf-2017-28, 2017
Manuscript under review for journal Earth Surf. Dynam.
Discussion started: 8 May 2017

3.1 End member model formulations

We have implemented two ways of determining whether enough lateral erosion has occurred to lower the lateral node. The first method dictates that the entire volume of the lateral node above the elevation of the downstream node must be eroded before its elevation is changed (Figure 1a,b). This formulation assumes that the bank material being eroded is resistant and/or blocky. This approach is used to represent, in a simple way, a system in which undermining of a channel bank leads to gravitational collapse of resistant material that must itself then be eroded in place (Lancaster, 1998). The second method dictates that only the volume of the water height on the bank times the cell area must be eroded for the elevation to change (Figure 1c,d). This model represents lateral erosion on a bank that has been laterally undercut and the remaining material slumps into the channel and is transported away as wash load, and assumes that the bank material slumps easily and rapidly breaks down into small grains that are easily transported. With these two end member models, we address whether lateral erosion rate should scale with valley wall height. In the first method, the total block erosion model, lateral migration depends on bank height so that taller banks experience slower lateral migration, as all of the volume of the lateral node must be eroded for the valley to widen (Lancaster, 1998). On the other hand, if all of the material that has been undercut by the channel is also swept away by the channel, then lateral erosion rate is independent of bank height. However, this undercutting-slump model is not appropriate for landscapes with very hard bedrock (low erodibility), as evidenced by overhanging cliffs along many rivers and persistent blocks of collapsed material following slumping or delivery from adjacent hillslopes (Shobe et al., 2016).

4 Model experiments

In order to explore the factors that control lateral bedrock erosion and valley widening, we ran sets of models using a range of values for bedrock erodibility, α (sediment mobility number), and K_l/K_v ratio using both the total block erosion model and the undercutting-slump model (Table 1). The model domain was 600 m by 600 m with 10 m cell size, three closed boundary edges and uplift rate relative to baselevel of 0.0005 m/yr imposed on the entire model domain. All models were spun up to an initial condition of approximately uniform erosion rate with vertical incision only. The models were then run for 100–200 ky with the lateral erosion component. In order to isolate the effect of bedrock erodibility, a set of model calculations were run where erodibility ranged from $5{\times}10^{-5}$ to $2.5{\times}10^{-4}$ while α was held constant at 0.8. In order to isolate the effect of detachment-limited vs. transport-limited behavior, another set of models was run where erodibility was held constant at $1{\times}10^{-4}$ and α values ranged from 0.1 to 2, which represents a detachment-limited system when $\alpha < 1$ and a transport-limited system when $\alpha > 1$ (Table 1). K_l/K_v ratios for all model runs were set to 1.0 or 1.5, resulting in a runoff rate of 14 mm/hr or 36 mm/hr from Equ. 13. Water flux was introduced in the top of the model by designating a node as an inlet with an area of 20,000 m^2 and sediment flux at carrying capacity so that each model run would have a primary channel on which to measure width and channel mobility.

Understanding the model behavior in response to detachment- vs. transport-limited behavior (represented by α) and K_l/K_v ratio is complex and requires understanding how runoff plays into both parameters. The value of α is calculated by v_s, a proxy for grain size, and runoff rate, R, although neither grain size nor runoff is explicitly set in the model runs. Values of α that

Earth Surf. Dynam. Discuss., doi:10.5194/esurf-2017-28, 2017
Manuscript under review for journal Earth Surf. Dynam.
Discussion started: 8 May 2017

capture a range of detachment- or transport-limited behavior is set instead (α=0.2–2.0). When K_l/K_v ratio is set for a given model (either 1.0 or 1.5 in all model runs), the runoff rate is calculated inside the model. Once a runoff rate for given K_l/K_v ratio is calculated, by extension, a value of v_s can be calculated from runoff rate and the set α value. Therefore, in model runs with the same K_l/K_v ratio and therefore the same runoff rate, a transport-limited system (α greater than 1) has a larger grain size (approximated by v_s) compared to a detachment-limited system with a low α.

Table 1. Model runs and parameters discussed in this paper.

model version	K_l/K_v	K	α	number of runs
total block	1.0–1.5	1×10^{-4}	0.2–2.0	10
total block	1.0–1.5	5×10^{-5}–2.5×10^{-4}	0.8	10
undercutting-slump	1.0–1.5	0.0001	0.2–2.0	10
undercutting-slump	1.0–1.5	0.00005–0.00025	0.8	10
TB water flux	1.0–1.5	0.00005–0.0025	0.8	6
UC water flux	1.0–1.5	0.00005–0.0025	0.8	6
TB sed flux	1.0–1.5	0.0001	0.2–2.0	10
UC sed flux	1.0–1.5	0.0001	0.2–2.0	10

4.1 Measures of lateral erosion in model landscapes

4.1.1 Channel mobility

Channel mobility distinguishes models with lateral erosion from models with only vertical incision. At steady state, channels in models with only vertical bedrock incision do not migrate across the model domain. However, a mobile channel is necessary to carve wide valleys and it is enticing to say that the more mobile the channels, the wider the valley will be. The effect of bedrock erodibility and α on channel migration through time for both model versions is shown in Figure 2. Channel migration over 200 ky is shown for six selected runs that span the range of bedrock erodibility and α values for the two different model formulations: the undercutting-slump model where K_l/K_v=1.5 and the total block erosion model where K_l/K_v=1.5. In all runs, the total block erosion model produced more confined channels compared to the undercutting-slump model. The undercutting-slump model produces more dynamic channel migration over the model domain, especially in the high K model. In both model formulations, the high K and high α runs have the widest extent of channel migration (recall that high α represents lower sediment mobility) and the low K and low α runs have the most restricted channel migration.

In order to describe channel mobility in our model runs in a single term, we calculate a cumulative migration metric, λ. λ is calculated by first determining the migration distance of the channel between time steps at all model cells the main channel

Earth Surf. Dynam. Discuss., doi:10.5194/esurf-2017-28, 2017
Manuscript under review for journal Earth Surf. Dynam.
Discussion started: 8 May 2017

occupies. Most often the migration distance between time steps at a single cell will be 0 or 10 m, indicating no migration or migration to a neighboring cell. The mean of migration distances between time steps is taken and summed over the duration of the model run to give the cumulative migration metric. λ, indicates how often the channel has migrated during the model run; a model run can have the same λ value if the channel marches across the entire model domain or if the channel repeatedly switches between two nearby channel courses. λ can also be used as an indicator for the maximum lateral extent occupied by the channel during the model run. That is, the extent of x positions occupied by the channel is λ at a maximum, but the actual x distance occupied by the main channel could be lower as the channel migrates over the same area repeatedly.

Bedrock erodibility and K_l/K_v ratio have the strongest control on channel migration distance. Channel mobility increases as bedrock erodibility increases in both the total block erosion model and the undercutting-slump model (Figure 3a,b). When K is low, representing strong bedrock lithology, there is limited channel movement in the total block erosion models with λ values between 15–35 m. This means that on average during the model run the channel occupied 1–3 cells (Figure 2c). With low values of K, the undercutting-slump model had λ values around 200 m, but a lateral extent of only 5 model cells (Figure 2c). This indicates that in the undercutting-slump model, the channel was actively migrating within a small area of the model domain. In model runs with high K values representing weak bedrock, total channel migration, λ increases, as well as the spatial extent of the channel migration (Figure 2a). With the total block model, λ appears to be a good proxy for total spatial extent of channels, but for the undercutting-slump model, λ tends to over estimate lateral extent of channel occupation (Figure 2).

Increasing the K_l/K_v ratio from 1.0 to 1.5, results in 1.5–2 times more channel mobility, with the largest relative increases in total block erosion model runs with high erodibility and higher α values (Figure 3a,b). This is because the undercutting-slump models already have high channel mobility with K_l/K_v equal to 1. Increasing K_l/K_v ratio to 1.5 increases channel mobility in UC models, but the total block erosion models have a larger threshold for lateral erosion so the increased K_l/K_v ratio results in relatively more channel mobility in the total block models.

For model runs with the same bedrock erodibility, but different α values (which represents sediment mobility), channel mobility is lower in models with lower values of α (representing high sediment mobility) and higher when $\alpha > 1$ (representing less mobile sediment) (Figure 3b). This effect is most pronounced in the total block erosion models, where channel mobility increases by a factor of four as α increases. In the undercutting-slump models, channel mobility also increases with α, especially when $K_l/K_v = 1.5$. When $K_l/K_v = 1$ in the undercutting-slump models, the trend in channel mobility vs. α is less well defined.

4.1.2 Valley width

Valley width is the primary indicator of lateral erosion; a wide bedrock valley implies that significant lateral erosion has occurred. Valleys can be defined in a few different ways; valley width needs to be quantified in our model. Many studies use low gradient areas of a DEM to determine valley width (e.g., Brocard and Van der Beek, 2006; May et al., 2013). This gives the width for the valley bottom that has been shaped by channel processes, but excludes areas that have been recently shaped by channel processes and then reworked by hillslope processes. Another way to measure valley width is by determining the

Earth Surf. Dynam. Discuss., doi:10.5194/esurf-2017-28, 2017
Manuscript under review for journal Earth Surf. Dynam.
Discussion started: 8 May 2017

width of the valley at a certain height above the channel. This simple metric is often used for finding valley width in the field, for example using eye height above the channel (e.g., Snyder et al., 2003a; Whittaker et al., 2007). Using a certain height above the channel to determine valley width in the models cannot distinguish between a fluvially carved bedrock valley and low relief in a landscape with weak bedrock. Instead we define valley width as the width of the area next to the main channel, where slope is characteristic of the fluvial channel rather than hillslopes for a given bedrock erodibility and α value. The reference slope for a fluvial channel is given by the slope-area relationship, assuming that the height of the landscape and Q_s are steady in time. When the height of the landscape is in equilibrium, Equations 1 and 3 are combined and rewritten as:

$$U = e - \frac{\nu_s d_* Q_s}{RA} \tag{14}$$

At steady state, Q_s is the total upstream eroded material, given by $Q_s = AU$. Substituting the steady state equation for Q_s and Equation 7 into Equation 14 gives

$$U = K_v A^{1/2} S - \alpha U \tag{15}$$

Solving the above equation for S gives the equation for reference slope that determines whether a model cell is shaped by fluvial or hillslope processes.

$$S = \frac{U}{K_v A^{1/2}}(\alpha + 1) \tag{16}$$

Our models successfully produce bedrock valleys that are several model cells wider than the channels that created them (Figure 4). Models with only vertical incision have v-shaped valleys that are only 1 model cell wide (10 meters in our experiments) and the channels do not shift laterally (Figure 4a). Given the specifications of the total block and undercutting-slump models, it is not surprising that valleys in the total block models take longer to respond to lateral erosion and are more narrow than in the undercutting-slump models. The total block erosion models take on the order of 10 ky to respond to lateral erosion and produce bedrock valleys that are up to 25 meters wide, while the undercutting-slump models take about 5 ky to respond to lateral erosion and produce valleys that are up to 50 m wide.

Figure 5 shows slope maps of total block and undercutting-slump models that show the width of the valley shaped by fluvial processes. The blue areas have slopes that are characteristic of fluvial channels and red areas have slopes that are characteristic of hillslopes. The total block erosion model with a low α value shows very little bedrock valley widening as evidenced by the thin band of blue along the main channel 1–2 model cells wide (Figure 5a). Increasing transport-limited behavior (higher α) results in wider valleys that have been shaped by the channel that are 2-3 model cells wide in the total block erosion model (Figure 5b). The landscape in the undercutting-slump model has wider valleys that result from more extensive carving by channels. The fluvially carved valleys in the detachment-limited model are about 2-3 model cells wide and the valleys in the transport-limited model are over 50 meters wide in some places (Figure 5c,d).

Figure 3c,d shows valley width for the lower two-thirds of the model channels averaged over the duration of the model runs in 54 model runs. To ensure that using characteristic fluvial slope as the criterion for a valley in all model runs gives valley width

Earth Surf. Dynam. Discuss., doi:10.5194/esurf-2017-28, 2017
Manuscript under review for journal Earth Surf. Dynam.
Discussion started: 8 May 2017

resulting from lateral erosion, and not valley width inherent in the model, we first use this criterion to measure valley width for the spin up models that include no lateral erosion component. Valley width for the spin up models is consistently 10 m, the width of one model cell. Valley width does not change significantly for any of the total block model runs in which K is varied and α is held constant (Figure 3c). When the K_l/K_v ratio is increased from 1 to 1.5, valley width increase slightly for all model runs, but wide valleys are not possible in the total block erosion model with this value of α. Valley width in the undercutting-slump model for changing bedrock erodibility shows a somewhat counter-intuitive signal (Figure 3c); the undercutting-slump model results in wider valleys for lower values of bedrock erodibility. The reasons for this signal are discussed in the section below.

When α is varied and K is constant, valley width increases with the tendency towards transport-limited conditions ($\alpha >$1) in all undercutting-slump models, but only in total block erosion models when the K_l/K_v ratio is equal to 1.5 (Figure 3b). The widest valleys for a given bedrock erodibility occur with high α values as a result of higher slope. The models predict more channel mobility and wider valleys under transport-limited streams (set by α) compared to detachment-limited streams (Figure 3b,d). As α increases, the deposition term increases, and a steeper slope is needed to maintain the landscape in steady state relative to uplift. Higher channel slopes in transport-limited model runs also cause increased lateral erosion according to equation 12.

4.1.3 Linking channel mobility and valley width

We have shown that the greatest channel mobility occurs in the undercutting-slump models and increases significantly with increasingly soft bedrock (Figure 3a). However, maximum channel mobility does not translate into maximum valley width. In the undercutting-slump models, the widest valleys occur in the low erodibility model runs that have relatively low channel mobility. This reflects that the areas visited by the migrating channel in the high K model runs is easily over-printed by hillslope processes due to its low relief. This prevents our algorithm from finding where an area of the model has recently shaped by the channel. The mismatch between channel mobility and valley width also reflects that hard bedrock valleys are allowed to erode very easily in the undercutting-slump model and the channel smoothed surface is persistent through time. The relationship between hard bedrock and wide valleys reflects the use of the undercutting-slump model, which is inappropriate for hard bedrock wall erosion in natural systems. With the undercutting-slump model, only a small volume threshold must be overcome for lateral erosion to occur, and the rest of the node material is transported downstream as wash load. However, it is these models that have resistant bedrock (low K) that are least suitable for the undercutting-slump model. In order for this to be a good description of how nature works, the bed material would need to be able to break up into small pieces that are easily transported away. The total block erosion model is more appropriate for representing the erosion of hard bedrock channels.

Earth Surf. Dynam. Discuss., doi:10.5194/esurf-2017-28, 2017
Manuscript under review for journal Earth Surf. Dynam.
Discussion started: 8 May 2017

4.2 Adding complexity: water flux, sediment flux

4.2.1 Effects of increased discharge on lateral channel migration

In order to investigate how transience in landscapes affects lateral erosion, we introduce increased discharge at the inlet point in the upstream end of the model. Using drainage area as a proxy for discharge, increasing water flux in the model represents how a larger stream on the same landscape will influence valley width. Increasing drainage area also allows us to observe the extent of landscape change and how rapidly the different model runs respond to an event such as stream capture. The drainage area at this input point is increased from 20,000 m^2 to 160,000 m^2 and sediment load is set to the carrying capacity of the new drainage area. For a typical model run, the additional drainage area approximately doubles the drainage area at the outlet of the main channel in the model domain. Models with increased water flux were run using both model formulations, $K_l/K_v = 1.0$ and 1.5, and erodibility values that ranged from 5×10^{-5}–2.5×10^{-4}, with alpha held constant at 0.8 (Table 1).

Recall that lateral erosion scales with drainage area (Equation 12), while vertical incision scales with the square root of drainage area (Equation 7), and therefore we expect that increasing drainage area will increase lateral erosion and valley width in every case for the undercutting-slumping model, where the threshold for lateral erosion is much smaller than in the total block erosion model. In the total block erosion model, lateral erosion will temporarily stall because of the volume threshold that must be exceeded before lateral erosion occurs. There is no threshold for vertical incision, which will speed up when additional water flux is added to the model.

4.2.2 Total Block erosion models

In all of the model runs, increased water flux resulted in increased lateral erosion and wider valleys. Figure 6 shows valley width averaged over the lower half of the model domain vs. model time for all of the water flux models. The total block erosion model and undercutting-slump model respond differently to a step change in water flux. The total block erosion models first incise vertically to a new steady state stream profile, then erode laterally as a result of the increased water flux, while the undercutting-slump model incise vertically and erode laterally simultaneously.

Total block erosion models where the K_l/K_v ratio is equal to 1.5 (TB1.5) show an interesting pattern in valley widening after increased water flux (Figure 6b). All of the TB1.5 model runs show a significant increase in valley width during the 50 ky period of increased water flux. After 6 ky of increased water flux (model time = 106 ky), the high and medium erodibility model runs have greater valley widths, but the low erodibility model shows a gradual increase in valley width over 14 ky of increased water flux (model time 100-114 ky). For the first 14 ky of the increased water flux, the channel of the low K model run incises rapidly, increasing the gradient between the channel and the adjacent cells and preventing lateral erosion. After the channel profile comes into new equilibrium, the increased water flux accelerates lateral erosion on the valley walls and valleys widen by 10 m compared to before increased water flux in the total block erosion models.

After the increased water flux stops at 150 ky, the wider valleys persist in the low and medium erodibility models (Figure 6b) for two reasons. First, after the cessation of increased water flux, the channel returns to equilibrium through aggradation and uplift. While aggradation is occurring, lateral erosion can occur more easily in the total block erosion models. In this case, the total volume that must be eroded from any lateral node cell is reduced as the channel floor moves up in vertical space. The second reason for persistent wide valleys is that in the medium and low K model runs, the increase in water flux eroded wide valleys into relatively resistant bedrock. These flat surfaces near the channel persist in harder bedrock, even after water flux has decreased to original levels. Following end of the period of increased water flux, valley width in the the TB1.5 medium K model run remains elevated for 10 ky (model time 160 ky), before channel narrowing that propagates upstream (Figure 7). After cessation of the increased water flux at 150 ky, the channel profile returns to equilibrium through uplift and aggradation (Figure 7a). Channel aggradation begins at the bottom of the channel profile and results in a convexity that propagates upstream (Figure 7a). At model position y=400, from 150–158 ky, the channel increases in elevation due to uplift (Figure 7b). Wide valleys created during increased water flux are maintained, and new lateral erosion of valley walls is seen (Figure 7b). At 159 ky, 9 ky after the cessation of increased water flux, the aggradational knickpoint reaches y=400 and incision and valley narrowing is observed (Figure 7d,e).

Figure 8a,b shows surface topography and cross sections across the model domain for two times in the low erodibility model run using the total block erosion model. This figure demonstrates the effect of valley deepening, then widening in response to increased water flux. Before water flux is increased, the channel is narrow and has steep valley walls (Figure 8a, Figure 9a,b). After 20 ky of increased water flux and increased vertical incision, channel erosion and baselevel fall reach a new equilibrium and channel elevation is stationary. Only after this period of re-equilibration can lateral erosion begin to widen the valleys. After 30 ky of increased water flux, the entire channel has incised, especially in the upper valley. At y=420, the position of the cross section, the channel has been incised by 3 m, and the valley has widened to about 20 m (Figure 8b). This response of primarily vertical incision is expected when using the total block erosion model, which sets a high threshold for lateral erosion.

4.2.3 Undercutting-slump models

In the undercutting-slump models, all of the model runs show a significant increase in channel mobility with additional water flux (Figure 6c,d). The largest valley widths occur in the models with low bedrock erodibility for reasons discussed above. Unlike the total block erosion models, there is no discernible lag between onset of water flux and valley widening in the undercutting-slump models. This is because the volume that must be eroded from neighboring nodes is set by the water surface height in this model formulation and the increase in drainage area increases lateral erosion rates more than vertical incision rates. Figure 8c,d shows topography and cross sections for two time in the low erodibility model run using the undercutting-slump model. Before water flux is increased, the channel is significantly wider than in the total block erosion model. The cross section shows a wide valley spanning three model cells, and low gradient areas on the neighboring interfluves, indicating that these areas were shaped by the lateral erosion from the channel. After 40 ky of increased water flux, the valley is much wider across the entire model domain, especially at the upstream segments of the channel. At y=420, the channel migrated 50 m across the model domain in 40 ky. The undercutting-slump model runs with medium and low erodibility maintain increased valley width after water flux has decreased, particularly in $K_l/K_v = 1.5$ models (UC1.5) (Figure 6d). This indicates that wide valley floors can persist for long periods of time after the conditions that created them have stopped.

Earth Surf. Dynam. Discuss., doi:10.5194/esurf-2017-28, 2017
Manuscript under review for journal Earth Surf. Dynam.
Discussion started: 8 May 2017

4.2.4 Effects of increased sediment flux on lateral erosion

In order to explore how the addition of sediment to a stream affects lateral erosion and valley widening, we added sediment to the inlet point at the top of the model. The sediment flux models were run for 100 ky with 50 ky of standard lateral erosion followed by 50 ky of increased sediment flux. Before additional sediment flux was added, the sediment flux at the inlet was equal to the carrying capacity of the stream, which is equal to UA. Models with increased sediment flux were run using both model formulations, $K_l/K_v = 1.0$ and 1.5, and α values that ranged from 0.2–2.0, with bedrock erodibility held constant at 1×10^{-4} (Table 1). During the 50 ky periods of increased sediment flux, five times more sediment flux was added, forcing all of the streams to aggrade initially. Adding sediment increases the deposition term (Equation 3), which will result in aggradation if the model is initially in steady state, that is $e-d=U$. Aggradation in the channels continues until the channel slopes become steep enough to increase the vertical erosion term so that $e-d=U$ again, and the landscape is in a new equilibrium state.

Figure 10 shows valley width averaged over the upper half of the model domain (closest to the sediment source) plotted against model time. After sediment is added to the models, all of the model runs show a significant increase in valley width, except the low α model runs, which show little change in width. Valley width increases more and valleys stay wide for longer with higher values of α. Valleys are narrowest and least persistent through time in the TB1 model group (Figure 10a), and valleys are widest and most persistent through time in the UC1.5 model group (Figure 10d). Valley widths and duration of wide valleys after the addition of sediment are similar between the TB1.5 group and the UC1 group (Figure 10b,c).

The addition of sediment to these models results in channel aggradation and valley filling that accounts for a substantial fraction of measured increases in valley width for all of these model runs. It is not possible to distinguish between widening due to valley filling and widening due to bedrock wall retreat from this spatially averaged value of valley width. However, we know that the TB1 models have little lateral bedrock erosion during the runs with no additional sediment flux, as seen in valley widths from 0–50 ky of the model runs (Figure 10a). Therefore, the valley widening that occurs from the TB1 model group is from valley filling only (Figure 9c) (further discussion in section below). We then subtract the values of valley width through time for the TB1 group from the valley width through time for the other models runs to determine valley widening from lateral erosion alone.

Figure 11 shows the difference in width through time between the model groups with significant widening and the total block model $K_l/K_v = 1$ model group, which has valley widening only in response to valley filling. This reveals interesting behaviors of the model groups through time, both before and after the addition of sediment flux. In Figure 11, the first 50 ky of the model runs show the differences in width between the control model group (TB1) and the other model groups under normal lateral erosion conditions. Differences are greatest in the undercutting-slump $K_l/K_v = 1.5$ (UC1.5) group and smallest in the total block $K_l/K_v = 1.5$ (TB1.5) group. After the addition of sediment flux, not all runs in the model groups showed an increase in valley width compared to the control run. Lower values of α showed little or no increase in bedrock valley width after the addition of sediment flux. This is because channels in the low α runs (high sediment mobility) easily adapt to the increased sediment flux without significant or far-reaching changes to the channel slope. In the TB1.5 and UC1 model groups, α values of 0.8–1.0 tend towards increased variability in valley width following the addition of sediment flux, but no convincing signal of increased valley width, with the exception of model run $\alpha = 0.8$ in model group TB1.5 (Figure 11a). Model runs with $\alpha > 1.0$ tend to have valley widths that are 10–30 meters wider than would be expected from valley filling alone. This effect is small, but detectable in the TB1.5 model group (Figure 9d).

Figure 9c,d shows model cross sections through time for the TB1 model and the TB1.5 model with α=1.5. The TB1 model shows valley widening exclusively through valley filling after the addition of sediment. Other channels shown in the cross section (at 80 m and 250 m) are immobile and show little evidence of lateral erosion (Figure 9c). Figure 9d shows an example of simultaneous valley filling and significant bedrock erosion in the TB1.5 model group. Before the addition of sediment flux (t=50ky), the channel is 10 meters wide. After the addition of sediment to the model, the channel aggrades by 2.5 meters while also shifting 50 meters to the right, eroding a significant amount of bedrock valley wall over 12 ky.

The response to increased sediment flux in the UC1.5 model group is different from the responses in the UC1 and TB1.5 groups. In the UC1.5 group, increased valley width following increased sediment flux is more clearly defined for the low-medium α values and the highest α value shows increased valley width due to sediment filling rather than from lateral erosion (Figure 11c). It is interesting to note that mean valley width increases at 50 ky for all model runs, then declines to close to pre-sediment values by about 80 ky. Mean valley width begins to decline as the models come into steady state with the increased sediment flux, indicating that lateral erosion can most readily occur when the channel is in a transient, aggradational state.

Figure 12 shows the $\alpha = 1.5$ run from model group UC1.5, before and after added sediment flux that results in true bedrock valley widening. At 50 ky in the model run before the additional sediment is added, the valley in the upper half of the model domain (y=240) is flat and about 30 m wide (Figure 12a). Over 50 ky, sediment is added to the model and the channel aggrades for $\sim$20 ky before it comes into steady state, i.e., its slope is steep enough to carry the additional sediment load and aggradation stops. During the 20 ky of aggradation, this model run shows both retreat of the valley walls and channel aggradation. By 70 ky in the model run, the channel has aggraded by 5 meters and the valley is 50 m wide (Figure 12b). During this 20 ky period, the channel has migrated 50 m to the right, eroding the hillslope and forming steep valley walls.

Before the increase in sediment flux, all channels are in equilibrium by definition. Adding sediment to the inlet point in the models causes the channels to aggrade in all model runs, increasing the channel slope. This increase in channel slope increases the lateral erosion term and the vertical erosion term (Eqs. 7, 12); but while the channel is aggrading, vertical incision is effectively zero. Therefore, for the total block erosion models, most new lateral erosion should occur while the channel is aggrading, because the threshold volume that must be eroded becomes smaller when relief between the channel node and neighboring nodes decreases (Figure 1). Figure 10 shows that after sediment flux is added, there is a persistent increase in valley width for many model runs even after the channel profile has come into steady state with respect to the added sediment flux. The permanent increase in slope should result in higher lateral erosion rates, resulting in permanently wider valleys because the increased vertical incision rates that result from the higher slope is offset by increased deposition. This suggests the possibility that if a channel experiences increased slope through aggradation, then more lateral erosion occurs.

5 Discussion

5.1 Comparison among purely vertical incision models and end member lateral erosion models

This simple theory for lateral bedrock channel erosion combined with a landscape evolution model produces valleys that are several times wider than the channels they hold. The development of wide valleys is sensitive to the model formulation selected, which is discussed below. The widest valleys in this set of models occur in transport-limited model runs (high α values) when using the undercutting-slump model formulation. The undercutting-slump algorithm represents easily erodible bedrock allowing the development of wider bedrock valleys, as observed in many natural systems (e.g., Montgomery, 2004; Snyder and Kammer, 2008; Schanz and Montgomery, 2016). Wider bedrock valleys under conditions of relatively immobile sediment (high α value) (Figure 5) reflect conditions observed in natural systems, where wide bedrock valleys are considered a diagnostic feature of transport-limited streams (Brocard and Van der Beek, 2006).

The results presented here show that the lateral erosion component allows for mobile channels in all model runs (Figure 3a,b), even when the model has reached steady state, unlike models with vertical incision only which have stationary channels at steady state. The modeling experiments show that landscapes with highly erodible bedrock have the most mobile channels. In both model formulations presented, easily erodible bedrock allows greater channel mobility because the amount of lateral erosion that must occur to erode valley walls is lower in low-relief landscapes with easily eroded bedrock. The model also predicts more channel mobility and wider valleys in models with high values of α (low sediment mobility), especially in the total block erosion models.

Channel mobility is a critical factor in the development of wide bedrock valleys, because all of the erosion of the valley must be accomplished through erosion by the channel (e.g., Tomkin et al., 2003). The width of surfaces beveled by lateral erosion has been framed as a competition between channel mobility and relative rock uplift rate (Bufe et al., 2016). Channel mobility is also important because measures of channel mobility during periods of lateral planation can be used to validate lateral erosion in models. The mobility of river channels increases with increasing sediment flux (Wickert et al., 2013), which emphasizes the potential importance of high sediment load as a requirement for the development of wide bedrock valleys. Landscapes in weaker bedrock are more likely to have more channel mobility and wider valleys because in natural systems, rivers flowing through soft bedrock are also more likely to behave as transport-limited rivers, as a result of the increased sediment flux in the stream from the surrounding hillslopes and lower channel slopes in easily eroded bedrock.

The two model formulations presented here describe end member behavior for different widening responses in hard and soft bedrock. The total block erosion model, in which the entire volume of a neighboring node must be eroded before lateral erosion can occur, best describes the behavior of resistant bedrock. In the undercutting-slump model, the neighboring node need only be undercut over the area of the model cell before the remainder of the node is transported out of the model as wash load, and more accurately reflects behavior from weakly cohesive bedrock that tends to weather into small pieces, such as shale. The undercutting-slump model consistently produces wider bedrock valleys and more mobile channels than the total block erosion model because less lateral erosion is required to erode valley walls in the undercutting-slump model algorithm.

Earth Surf. Dynam. Discuss., doi:10.5194/esurf-2017-28, 2017
Manuscript under review for journal Earth Surf. Dynam.
Discussion started: 8 May 2017

The behavior of the models varies significantly based on which model is selected, although the same general trends are seen in both models. In nature, lateral erosion will not follow either one of these end members perfectly, but will operate on a continuum between the two (Lancaster, 1998). Tomkin et al. (2003) presented two end member relationships between channel erosion and valley erosion that are similar to the models presented here and they found similar behavior between their two models.

5.2 Comparison between models and field studies

Lateral erosion rates depend on the magnitude of shear stress and tools applied to channel walls, and the resistance of the bedrock to erosion. Our model of lateral bedrock erosion proposes that channel curvature controls lateral erosion rate. Cook et al. (2014) showed that extremely efficient bedrock wall erosion of up to ∼80 m over 5 years occurred where the river encountered sharp bends. They attribute this rapid lateral bedrock erosion in river bends to abrasion from sediment particles that detach from flow lines in the curve and impact the wall. Fuller et al. (2016) also suggest that lateral erosion rate by bedrock abrasion depends on how often sediment particles are deflected towards the channel walls.

The total block erosion model demonstrates how landscapes with hard bedrock and detachment-limited conditions respond to increased discharge by first incising the channel bed, and then widening after the channel has into equilibrium (Figure 9a,b). This behavior is similar to narrowing and incision of bedrock channels in response to increased uplift or increased discharge (Duvall et al., 2004). The model predicts that not only will channels in easily eroded bedrock reach equilibrium more quickly than channels in resistant bedrock, but channels in easily eroded bedrock will begin to widen valleys faster than in more resistant bedrock (Lavé and Avouac, 2001).

One of the few studies that has been able to report bedrock valley widening through time is from a unique case in Death Valley (Snyder and Kammer, 2008). Stream capture increased the drainage area of a small basin by 75 fold in the 1940's and channel response over the following 60 years was mapped by aerial photos. Snyder and Kammer (2008) found that mean valley width in a channel segment with weak bedrock increased by 9 meters in 60 years. In contrast, in channel segments in hard bedrock, they found vertical channel incision and the development of knickpoints. They attribute the difference in response to lithological differences and suggest that the presence of sediment on the bed in the weak bedrock channel segments protects the bed from incision, allowing the valley walls to migrate laterally. This difference in response is similar to the behavior of the end-member models presented here: the total block erosion model shows rapid incision and narrowing in response to increased water flux, whereas the undercutting-slump models show incision and valley widening.

In nature, we often assume that lateral erosion is achieved by adding sediment, suppressing vertical erosion and giving lateral erosion a chance to outpace vertical incision. If this is the case, then we expect increased sediment flux to have the largest effect on the low α/detachment-limited model runs. The same amount of new sediment was added to each model run, but the sediment resulted in more aggradation the high α runs. In the high α/transport-limited runs, the channels already behave as if they are loaded with sediment. In low α runs, the model tends towards detachment-limited behavior, so there is abundant stream power carry away the sediment. The slope needed to transport the additional sediment is lower in the detachment-limited runs, resulting in less aggradation in response to the increased sediment flux.

Earth Surf. Dynam. Discuss., doi:10.5194/esurf-2017-28, 2017
Manuscript under review for journal Earth Surf. Dynam.
Discussion started: 8 May 2017

The addition of sediment in this model does not lead to increased sediment cover on the bed, as bedrock and sediment are not differentiated in the model, but rather results in immediate channel aggradation. This channel aggradation in the model certainly indicates that vertical incision has stopped, allowing lateral erosion to become the primary erosive agent, even in models where K_l/K_v ratio is low or in the total block erosion models. This predicted increase in lateral erosion during periods of aggradation occurs in many of the model runs, especially those with high α values. When the channel has reached a new equilibrium following increased sediment flux, many model runs maintain wider valleys due to the higher slope and increased lateral erosion rates.

5.3 Model limitations

While the model captures several important markers of lateral bedrock erosion, the model did not develop broad, smooth, valleys that are many times the width of their channel and that are sustained over many years, as observed in flights of strath terraces in the Front Range of Colorado, for example. The model also did not show a strong relationship between increased sediment flux and protection of the channel bed from vertical incision and increased lateral erosion of valley walls. Some important elements of reality have been omitted or set with a lumped parameter in this model, such as 1) treating sediment and bedrock erodibility separately, 2) setting variability and magnitude of runoff separately from grain size, 3) threshold effects of sediment on bed, 4) hillslope processes, 5) differences in grain sizes, 6) changes in bank material through time from weathering or water content. The first three items are the most important in our opinion.

In order to focus on implementing the equations for lateral erosion into the model, the simplest possible erosion-deposition model was used. This erosion-deposition model (Equation 1) has the advantage of not requiring the calculation of transport capacity and prevents potential problems with abrupt transitions from erosion to deposition, but does so at the expense of losing the details of runoff rate and grain size, which are lumped into the parameter α. In this model, detachment- or transport-limited behavior is set through α, which works well for general model exploration, but becomes problematic when exploring specific model responses to changes in runoff rate and sediment size. Setting runoff and grain size explicitly is a important next step for determining how these factors independently impact bedrock valley width and channel mobility.

Another limitation of the current model is that sediment is not treated explicitly, but rather is tracked in the model through the Q_s term. No distinction in erodibility is made between sediment and bedrock. In the current model, when the landscape is in steady state, vertical erosion plus deposition is equal to the uplift rate. Increasing sediment flux, Q_s, in the deposition term immediately results in channel aggradation. In model formulations that use the concept of transport capacity of a stream, adding sediment to a river that is far below transport capacity will not cause aggradation, but will easily carry the sediment load downstream. If sediment is continually added to a such a stream, the ratio of sediment flux, Q_s, to transport capacity, Q_t, will increase until Q_s/Q_t=1 and the stream becomes transport-limited (Willgoose et al., 1991). As Q_s/Q_t for a stream increases, the bed of the stream is progressively covered by more sediment, protecting the underlying bedrock from further incision (Sklar and Dietrich, 2004). Under these kinds of scenarios, adding sediment to a detachment-limited stream eventually reduces vertical incision, and allows lateral erosion to widen the bedrock channel walls while the bed remains stationary (Hancock and Anderson, 2002).

Earth Surf. Dynam. Discuss., doi:10.5194/esurf-2017-28, 2017
Manuscript under review for journal Earth Surf. Dynam.
Discussion started: 8 May 2017

In not differentiating between sediment and bedrock explicitly in this model, the different erodibilities of sediment and bedrock are not accounted for. In most cases, sediment in a channel should be much easier to erode than the bedrock in a channel. But in some cases, sediment in a soft bedrock channel can be composed of coarse grained, resistant lithology sourced from upstream. For example, the streams that drain the Colorado Front Range flow from hard, crystalline bedrock onto soft, friable shale bedrock (Langston et al., 2015). The granitic cobbles that armor the channel bed in stream segments underlain by shale bedrock, take much more energy to move than it does to transport the friable flakes of shale that line the walls of the channel.

6 Conclusions

We have shown that a simple, physics-based theory for lateral bedrock channel migration, when combined with a landscape evolution model, produces several interesting behaviors observed in natural systems. During transient channel incision, lateral erosion in the model temporarily stalls until channel equilibrium is re-established. Following a transient disturbance, wide bedrock valleys develop more quickly in weaker bedrock. The model predicts wider bedrock valleys with easily erodible bedrock, as many have observed in natural landscapes (Montgomery, 2004; Brocard and Van der Beek, 2006). Weaker bedrock also results in more channel mobility, which is a fundamental factor for developing and maintaining a bedrock valley that is several times wider than the channel it holds (Tomkin et al., 2003). Increased channel mobility and wider flat-bottomed valleys under transport-limited conditions in the model, suggests that sediment cover on the bed that is present under transport-limited conditions is an effective way to slow vertical incision and amplify the effect of lateral erosion (Hancock and Anderson, 2002). However, the model lacks some important elements of reality, especially variations in runoff and separate handling of bedrock and sediment in the channels. Our theory for the lateral erosion of bedrock channel walls and the numerical implementation of the theory in a catchment-scale landscape evolution model is a significant first step towards understanding the factors that control the rates and spatial extent of wide bedrock valleys.

Code availability. The lateral erosion models described in this text will be made available as a Landlab component in the summer of 2017.

Competing interests. The authors declare that there are no competing interests present.

References

Andrews, E. D.: Bed-material entrainment and hydraulic geometry of gravel-bed rivers in Colorado, Geological Society of America Bulletin, 95, 371–378, 1984.

Barbour, J., Stark, C., Lin, C.-W., Chen, H., Horng, M.-J., Ko, C.-P., Yi, T.-C., Tsai, T.-T., Chang, W.-S., Lee, S.-P., et al.: Magnitude-frequency distributions of boundary shear stress along a rapidly eroding bedrock river, Geophysical Research Letters, 36, 2009.

Beer, A., Turowski, J. M., Kirchner, J. W., et al.: Spatial patterns of erosion in a bedrock gorge, Journal of Geophysical Research: Earth Surface, 122, 191–214, 2017.

Brocard, G. Y. and Van der Beek, P.: Influence of incision rate, rock strength, and bedload supply on bedrock river gradients and valley-flat widths: Field-based evidence and calibrations from western Alpine rivers (southeast France), Geological Society of America Special Papers, 398, 101–126, 2006.

Bufe, A., Paola, C., and Burbank, D. W.: Fluvial bevelling of topography controlled by lateral channel mobility and uplift rate, Nature Geoscience, 2016.

Chadwick, O. A., Hall, R. D., and Phillips, F. M.: Chronology of Pleistocene glacial advances in the central Rocky Mountains, Geological Society of America Bulletin, 109, 1443–1452, 1997.

Clevis, Q., Tucker, G. E., Lancaster, S. T., Desitter, A., Gasparini, N., and Lock, G.: A simple algorithm for the mapping of TIN data onto a static grid: applied to the stratigraphic simulation of river meander deposits, Computers & geosciences, 32, 749–766, 2006a.

Clevis, Q., Tucker, G. E., Lock, G., Lancaster, S. T., Gasparini, N., Desitter, A., and Bras, R. L.: Geoarchaeological simulation of meandering river deposits and settlement distributions: A three-dimensional approach, Geoarchaeology, 21, 843–874, 2006b.

Cook, K. L., Turowski, J. M., and Hovius, N.: River gorge eradication by downstream sweep erosion, Nature Geoscience, 7, 682–686, 2014.

Davy, P. and Lague, D.: Fluvial erosion/transport equation of landscape evolution models revisited, Journal of Geophysical Research: Earth Surface (2003–2012), 114, 2009.

Dühnforth, M., Anderson, R. S., Ward, D. J., and Blum, A.: Unsteady late Pleistocene incision of streams bounding the Colorado Front Range from measurements of meteoric and in situ 10Be, Journal of Geophysical Research: Earth Surface (2003–2012), 117, 2012.

Duvall, A., Kirby, E., and Burbank, D.: Tectonic and lithologic controls on bedrock channel profiles and processes in coastal California, Journal of Geophysical Research: Earth Surface (2003–2012), 109, 2004.

Finnegan, N. J. and Dietrich, W. E.: Episodic bedrock strath terrace formation due to meander migration and cutoff, Geology, 39, 143–146, 2011.

Fuller, T. K., Gran, K. B., Sklar, L. S., and Paola, C.: Lateral erosion in an experimental bedrock channel: The influence of bed roughness on erosion by bed load impacts, Journal of Geophysical Research: Earth Surface, 121, 1084–1105, 2016.

Gilley, J. E., Kottwitz, E. R., and Wieman, G. A.: Darcy-Weisbach roughness coefficients for gravel and cobble surfaces, Journal of irrigation and drainage engineering, 118, 104–112, 1992.

Hancock, G. S. and Anderson, R. S.: Numerical modeling of fluvial strath-terrace formation in response to oscillating climate, Geological Society of America Bulletin, 114, 1131–1142, 2002.

Hartshorn, K., Hovius, N., Dade, W. B., and Slingerland, R. L.: Climate-driven bedrock incision in an active mountain belt, Science, 297, 2036–2038, 2002.

Hin, L. S., Bessaih, N., Ling, L. P., Ghani, A. A., and Seng, M. Y.: Determination of apparent and composite friction factors for flooded equatorial natural rivers, International Journal of River Basin Management, 6, 3–12, 2008.

Johnson, J. P. and Whipple, K. X.: Evaluating the controls of shear stress, sediment supply, alluvial cover, and channel morphology on experimental bedrock incision rate, Journal of Geophysical Research: Earth Surface (2003–2012), 115, 2010.

Kirkby, M.: Landscape modelling at regional to continental scales, in: Process modelling and landform evolution, pp. 187–203, Springer, 1999.

Lancaster, S. T.: A nonlinear river meandering model and its incorporation in a landscape evolution model, Ph.D. thesis, Massachusetts Institute of Technology, 1998.

Langston, A. L., Tucker, G. E., and Anderson, R. S.: Interpreting climate-modulated processes of terrace development along the Colorado Front Range using a landscape evolution model, Journal of Geophysical Research: Earth Surface, 120, 2121–2138, 2015.

Lavé, J. and Avouac, J.: Fluvial incision and tectonic uplift across the Himalayas of central Nepal, Journal of Geophysical Research: Solid Earth (1978–2012), 106, 26 561–26 591, 2001.

Leopold, L. B. and Maddock, T.: The hydraulic geometry of stream channels and some physiographic implications: Professional Paper 252, Tech. rep., US Geological Survey, 1953.

Limaye, A. and Lamb, M. P.: A vector-based method for bank-material tracking in coupled models of meandering and landscape evolution, Journal of Geophysical Research: Earth Surface, 118, 2421–2437, 2013.

Limaye, A. and Lamb, M. P.: Numerical simulations of bedrock valley evolution by meandering rivers with variable bank material, Journal of Geophysical Research: Earth Surface, 119, 927–950, 2014.

May, C., Roering, J., Eaton, L., and Burnett, K.: Controls on valley width in mountainous landscapes: The role of landsliding and implications for salmonid habitat, Geology, 41, 503–506, 2013.

Montgomery, D. R.: Observations on the role of lithology in strath terrace formation and bedrock channel width, American Journal of Science, 304, 454–476, 2004.

Schanz, S. A. and Montgomery, D. R.: Lithologic controls on valley width and strath terrace formation, Geomorphology, 258, 58–68, 2016.

Shobe, C. M., Tucker, G. E., and Anderson, R. S.: Hillslope-derived blocks retard river incision, Geophysical Research Letters, 43, 5070–5078, 2016.

Sklar, L. S. and Dietrich, W. E.: A mechanistic model for river incision into bedrock by saltating bed load, Water Resources Research, 40, 2004.

Snyder, N. P. and Kammer, L. L.: Dynamic adjustments in channel width in response to a forced diversion: Gower Gulch, Death Valley National Park, California, Geology, 36, 187–190, 2008.

Snyder, N. P., Whipple, K. X., Tucker, G. E., and Merritts, D. J.: Channel response to tectonic forcing: field analysis of stream morphology and hydrology in the Mendocino triple junction region, northern California, Geomorphology, 53, 97–127, 2003a.

Snyder, N. P., Whipple, K. X., Tucker, G. E., and Merritts, D. J.: Importance of a stochastic distribution of floods and erosion thresholds in the bedrock river incision problem, Journal of Geophysical Research: Solid Earth (1978–2012), 108, 2003b.

Stark, C. P., Barbour, J. R., Hayakawa, Y. S., Hattanji, T., Hovius, N., Chen, H., Lin, C.-W., Horng, M.-J., Xu, K.-Q., and Fukahata, Y.: The climatic signature of incised river meanders, Science, 327, 1497–1501, 2010.

Suzuki, T.: Rate of lateral planation by Iwaki River, Japan, Trans. Jpn. Geomorphol. Union, 3, 1–24, 1982.

Tomkin, J. H., Brandon, M. T., Pazzaglia, F. J., Barbour, J. R., and Willett, S. D.: Quantitative testing of bedrock incision models for the Clearwater River, NW Washington State, Journal of Geophysical Research: Solid Earth (1978–2012), 108, 2003.

Tucker, G. and Hancock, G.: Modelling landscape evolution, Earth Surface Processes and Landforms, 35, 28–50, 2010.

Tucker, G. E. and Bras, R. L.: A stochastic approach to modeling the role of rainfall variability in drainage basin evolution, Water Resources Research, 36, 1953–1964, 2000.

Turowski, J. M., Lague, D., and Hovius, N.: Cover effect in bedrock abrasion: A new derivation and its implications for the modeling of bedrock channel morphology, Journal of Geophysical Research: Earth Surface (2003–2012), 112, 2007.

Turowski, J. M., Hovius, N., Meng-Long, H., Lague, D., and Men-Chiang, C.: Distribution of erosion across bedrock channels, Earth Surface Processes and Landforms, 33, 353–363, 2008.

Turowski, J. M., Lague, D., and Hovius, N.: Response of bedrock channel width to tectonic forcing: Insights from a numerical model, theoretical considerations, and comparison with field data, Journal of Geophysical Research: Earth Surface (2003–2012), 114, 2009.

Whipple, K. X. and Tucker, G. E.: Implications of sediment-flux-dependent river incision models for landscape evolution, Journal of Geophysical Research: Solid Earth (1978–2012), 107, ETG–3, 2002.

Whittaker, A. C., Cowie, P. A., Attal, M., Tucker, G. E., and Roberts, G. P.: Contrasting transient and steady-state rivers crossing active normal faults: New field observations from the Central Apennines, Italy, Basin Research, 19, 529–556, 2007.

Wickert, A. D., Martin, J. M., Tal, M., Kim, W., Sheets, B., and Paola, C.: River channel lateral mobility: metrics, time scales, and controls, Journal of Geophysical Research: Earth Surface, 118, 396–412, 2013.

Willgoose, G., Bras, R. L., and Rodriguez-Iturbe, I.: A coupled channel network growth and hillslope evolution model: 1. Theory, Water Resources Research, 27, 1671–1684, 1991.

Wobus, C. W., Tucker, G. E., and Anderson, R. S.: Self-formed bedrock channels, Geophysical Research Letters, 33, 2006.

Yanites, B. J. and Tucker, G. E.: Controls and limits on bedrock channel geometry, Journal of Geophysical Research: Earth Surface (2003–2012), 115, 2010.

Yanites, B. J., Tucker, G. E., Hsu, H.-L., Chen, C.-c., Chen, Y.-G., and Mueller, K. J.: The influence of sediment cover variability on long-term river incision rates: An example from the Peikang River, central Taiwan, Journal of Geophysical Research: Earth Surface, 116, 2011.

Earth Surf. Dynam. Discuss., doi:10.5194/esurf-2017-28, 2017
Manuscript under review for journal Earth Surf. Dynam.
Discussion started: 8 May 2017

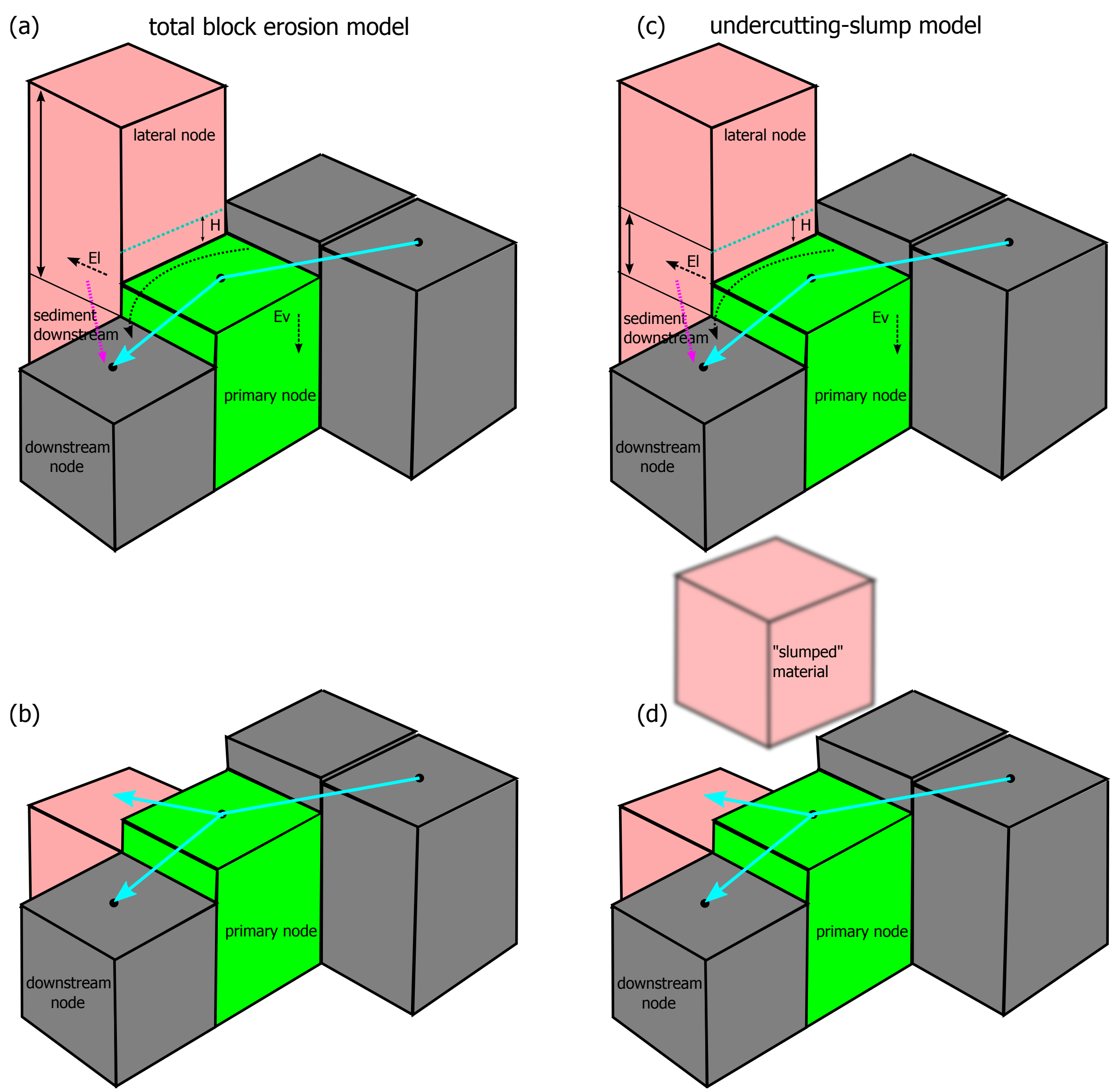

Figure 1. Conceptual illustration of model nodes showing the stream segments (in light blue) from the upstream node to the primary node (in green), to the downstream node. Vertical erosion (E_v) occurs at the primary node. The neighbor node (in pink) where lateral erosion (E_l) occurs is located on the outside bend of the stream segments. The height over which lateral erosion occurs, H, is shown in the dashed blue line. a) For the total block erosion model, the volume that must be laterally eroded before elevation is changed is $(Z_n - Z_d)dx^2$, the difference in elevation between the neighbor node and the downstream node (indicated with black arrow) times the surface area of the neighbor node. b) Elevation of the lateral node is changed after after the entire block is eroded and flow can (potentially) be rerouted. c) In the undercutting-slump model, the volume that must be laterally eroded (representing bank undercutting) before elevation is changed is $(H - Z_d)dx^2$. $H - Z_d$ is the difference in elevation between the water surface height and the elevation of the downstream node, indicated with black arrow. d) When the neighbor node has been undercut, elevation is changed, allowing water to be re-routed, while the slumped material is transported downstream as washload.

Earth Surf. Dynam. Discuss., doi:10.5194/esurf-2017-28, 2017
Manuscript under review for journal Earth Surf. Dynam.
Discussion started: 8 May 2017

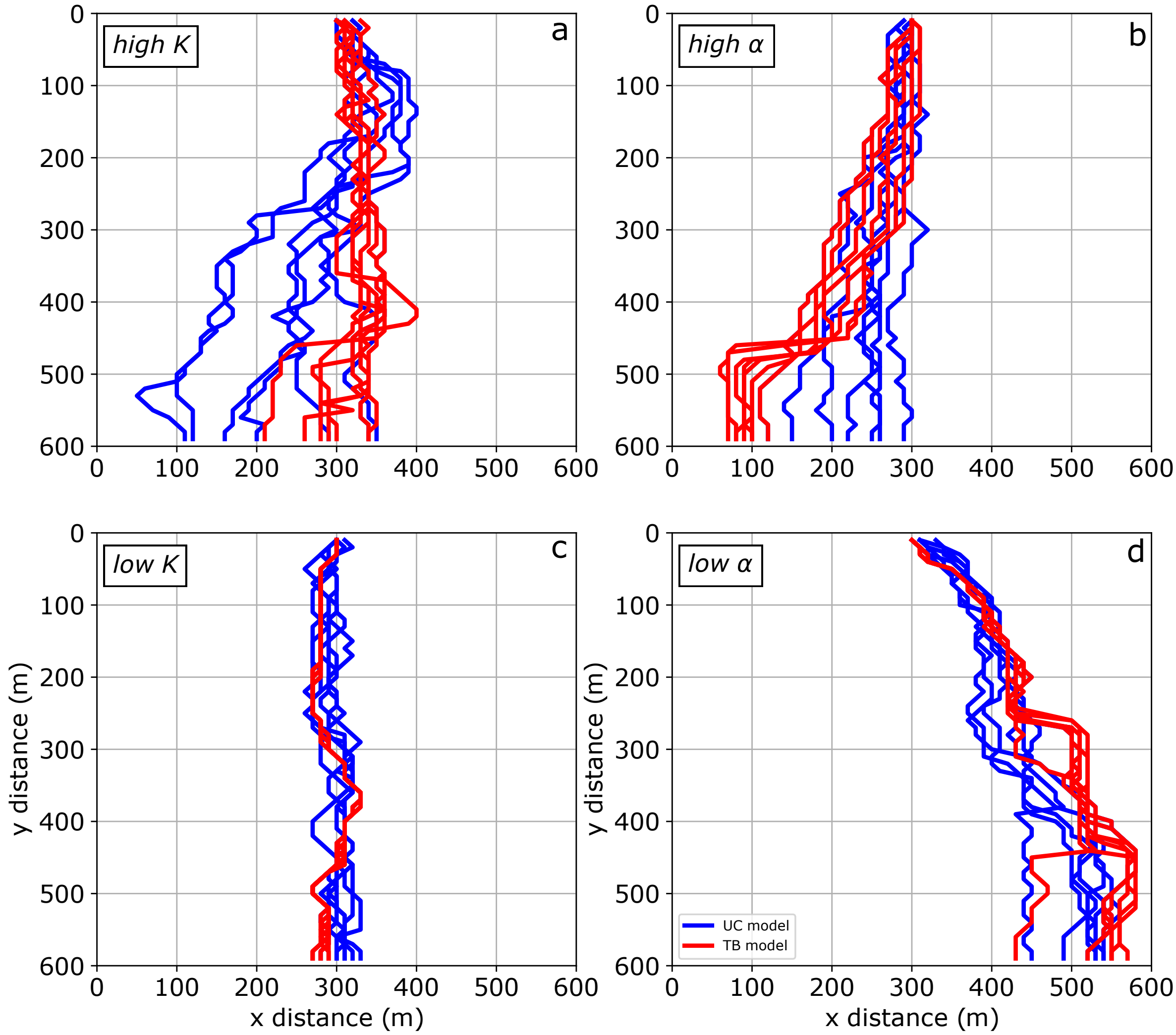

Figure 2. Channel positions over 200 ky with different values for bedrock erodibility and α in the undercutting-slump model (blue lines) and total block erosion model (red lines). a) high bedrock erodibility, medium α value. b) high α (low sediment transport), medium bedrock erodibility. c) low bedrock erodibility, medium α value. d) low α (high sediment transport), medium bedrock erodibility.

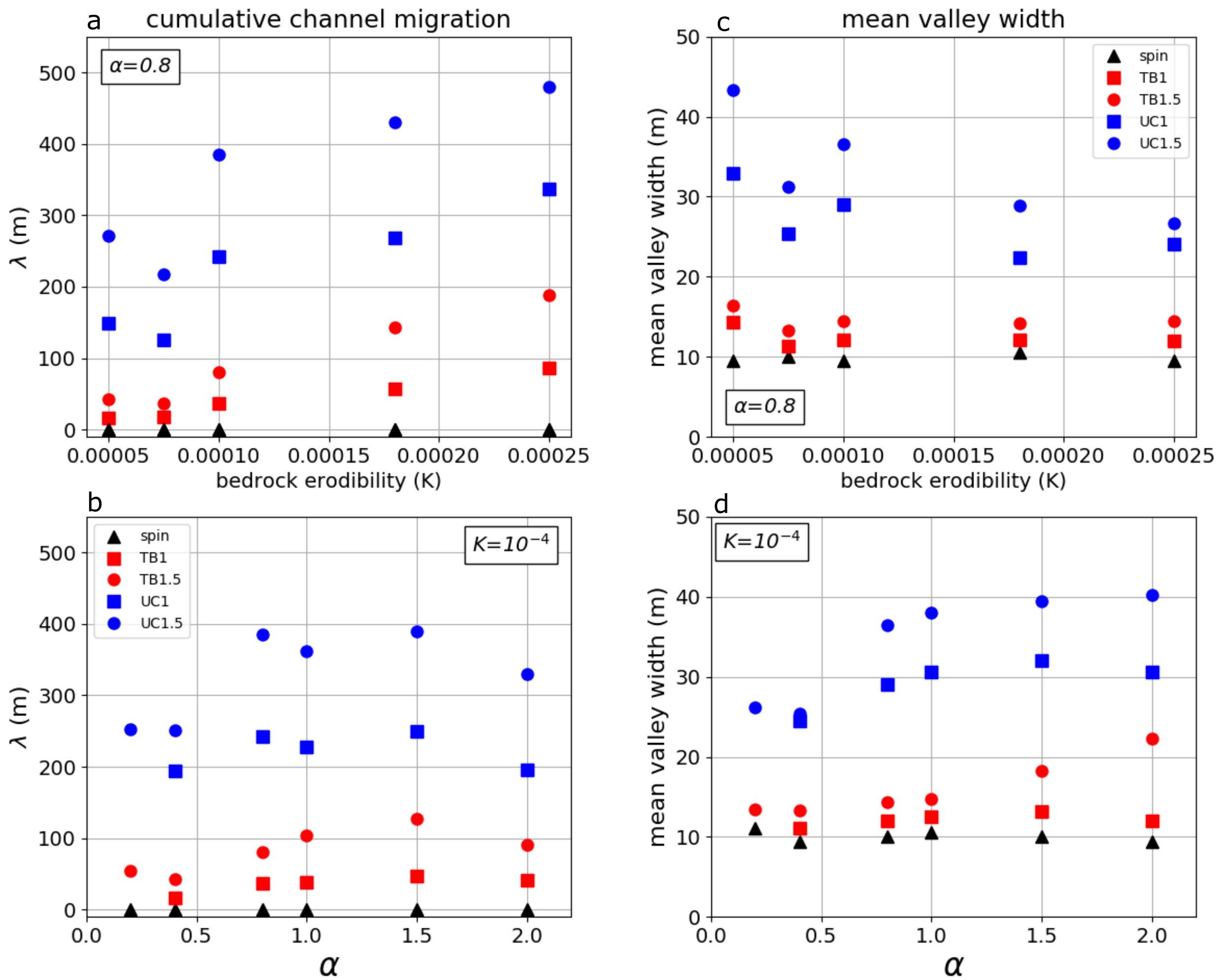

Figure 3. Cumulative channel-averaged migration (a,b) and mean valley width (c,d) over 100 ky for total block erosion models and undercutting-slump models with $K_l/K_v = 1$ and 1.5. a) Cumulative channel-averaged migration (λ) for model runs with $\alpha = 0.8$ plotted against bedrock erodibility, K. b) λ for model runs with $K = 10^{-4}$ plotted against α. Mean valley width averaged over 100 ky of the model runs. c) Mean valley width for model runs with $\alpha = 0.8$ plotted against bedrock erodibility, K. d) Mean valley width for model runs with $K = 10^{-4}$ plotted against α.

Earth Surf. Dynam. Discuss., doi:10.5194/esurf-2017-28, 2017
Manuscript under review for journal Earth Surf. Dynam.
Discussion started: 8 May 2017

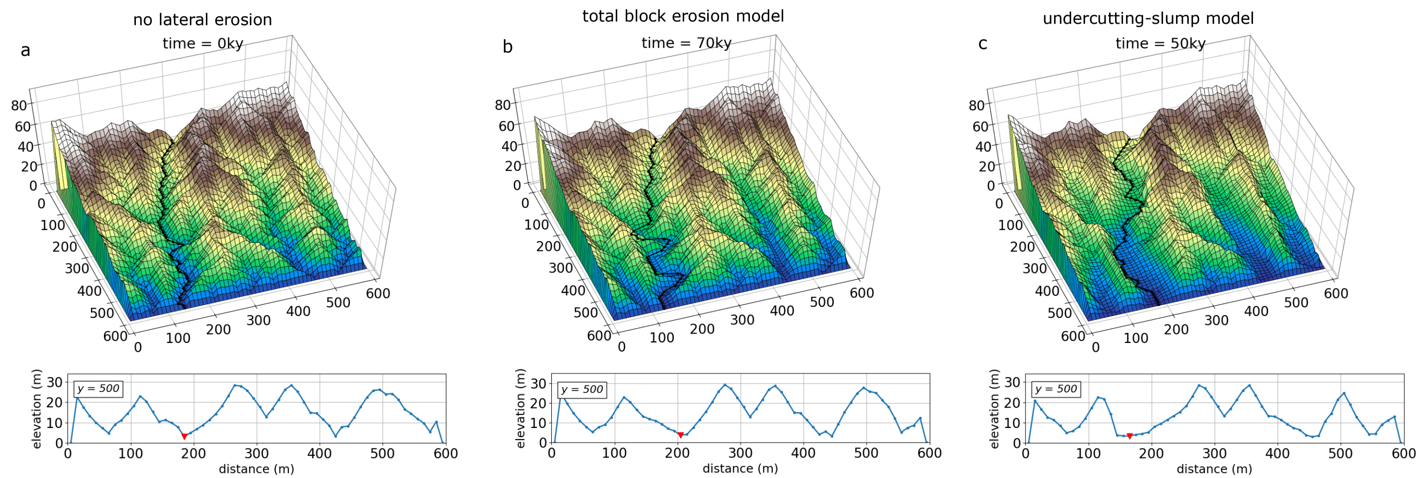

Figure 4. Model topography and cross sections at y=500 showing examples of valley widening. Black line indicates position of the main channel on the landscape. Red triangle shows position of the main channel in the cross section. a) Model with vertical incision only. b) Total block erosion model after 70 ky of lateral erosion. c)Undercutting-slump model after 50 ky of lateral erosion.

Earth Surf. Dynam. Discuss., doi:10.5194/esurf-2017-28, 2017
Manuscript under review for journal Earth Surf. Dynam.
Discussion started: 8 May 2017

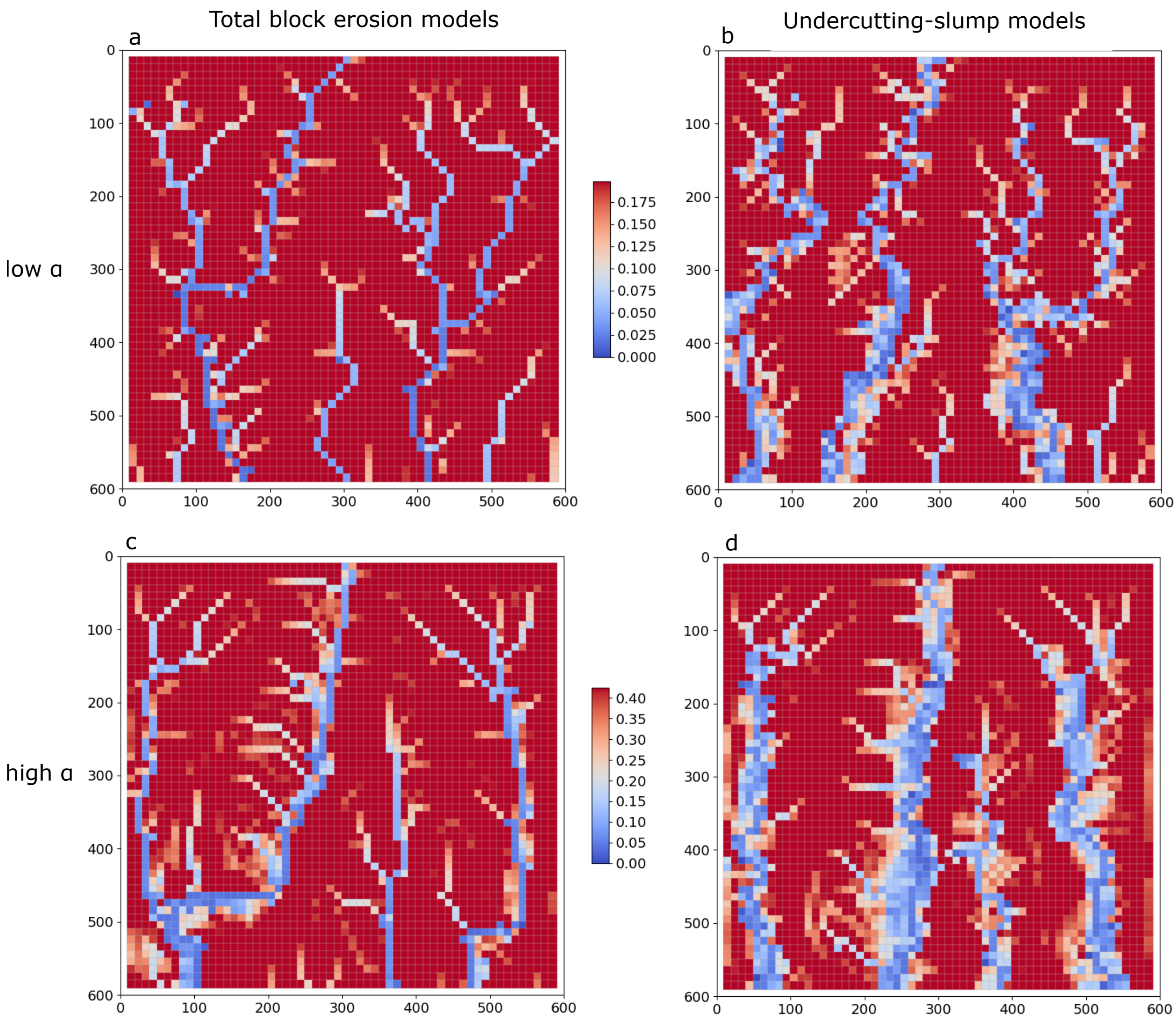

Figure 5. Slope maps showing fluvially carved valleys in total block erosion and undercutting-slump models with high and low values of α. The white and blue areas in the maps that indicate slopes that are characteristic of fluvial channels, i.e. lower than the reference slope value (Equation 16). a. Total block erosion model, low α (detachment-limited) b. Undercutting-slump model, low α (detachment-limited) c. Total block erosion model, high α (transport-limited) d. Undercutting-slump model, high α (transport-limited)

Earth Surf. Dynam. Discuss., doi:10.5194/esurf-2017-28, 2017
Manuscript under review for journal Earth Surf. Dynam.
Discussion started: 8 May 2017

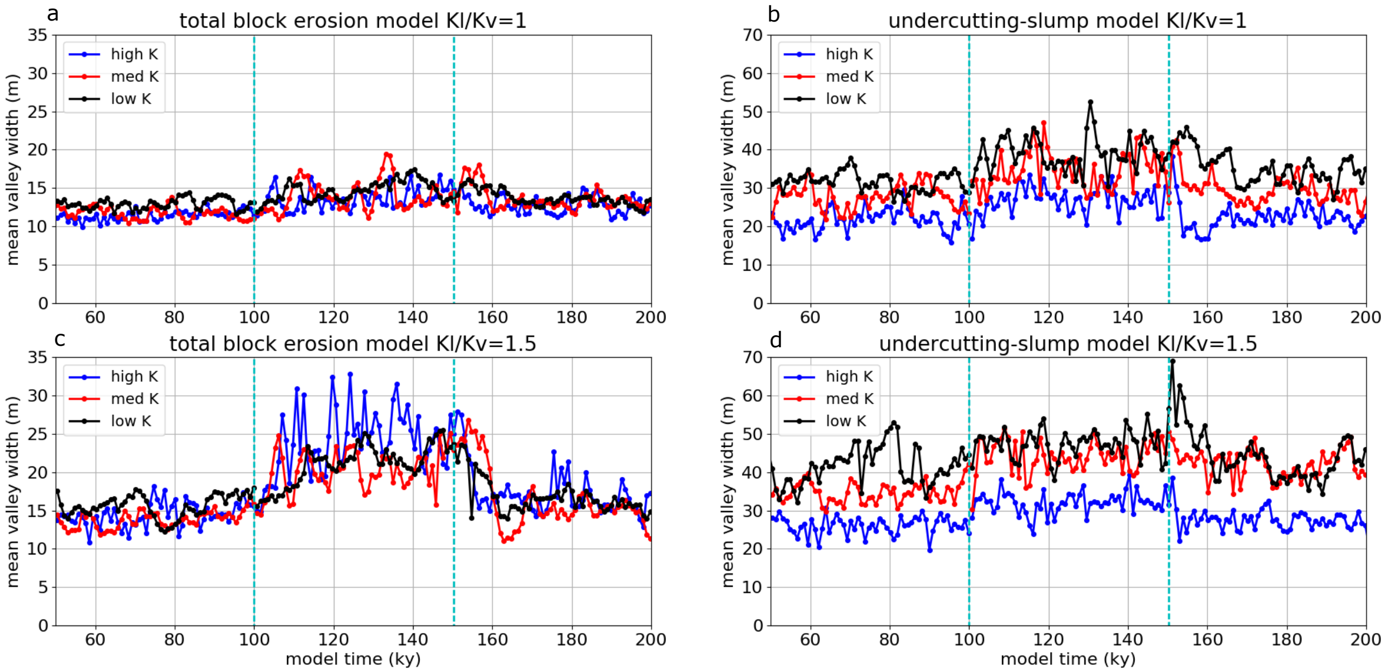

Figure 6. Valley width averaged over the upper half of the model domain vs. model time for total block erosion and undercutting-slump models with $K_l/K_v =$ to 1 and 1.5. Water flux occurs from 100 ky to 150 ky, indicated by dashed lines.

Earth Surf. Dynam. Discuss., doi:10.5194/esurf-2017-28, 2017
Manuscript under review for journal Earth Surf. Dynam.
Discussion started: 8 May 2017

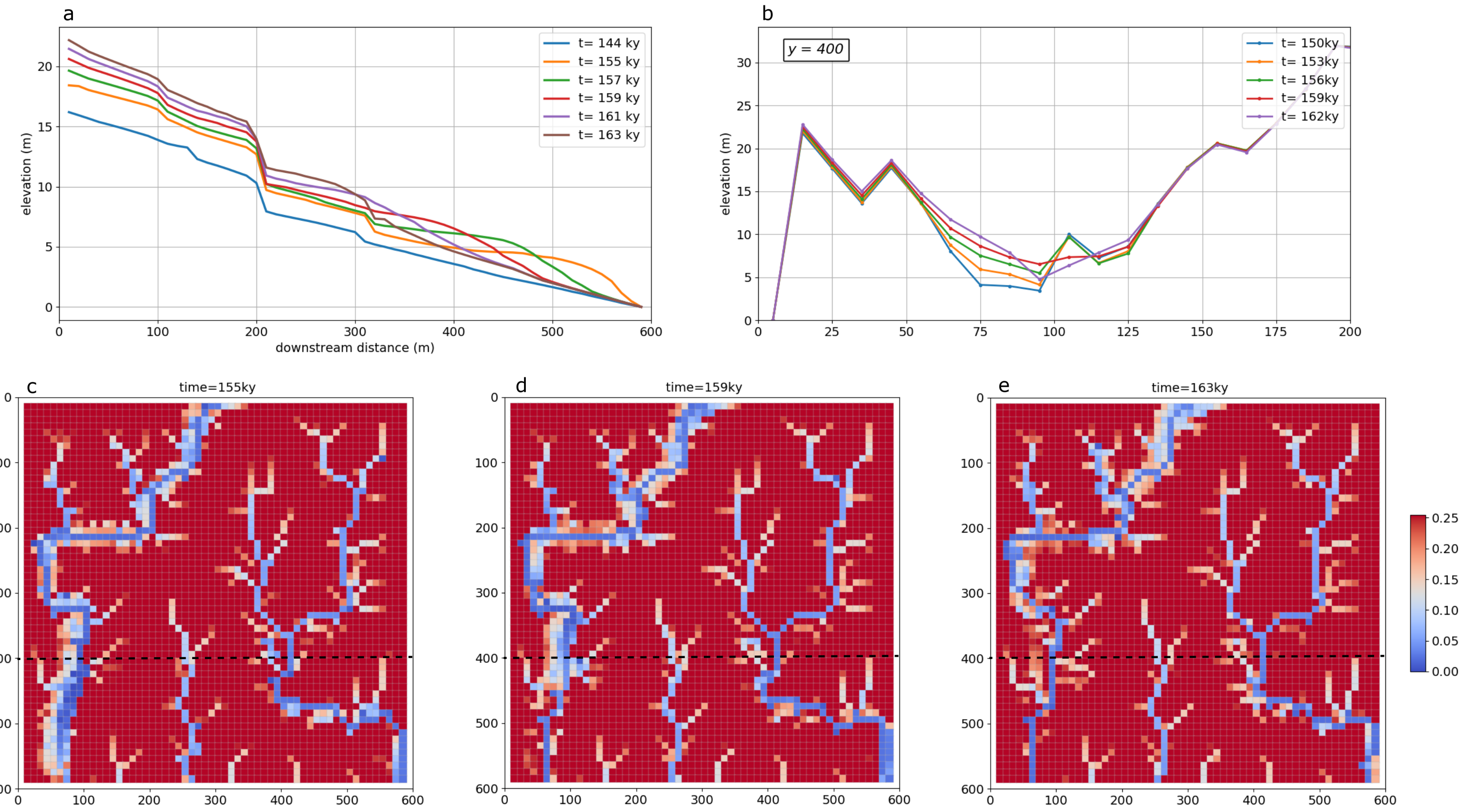

Figure 7. Longitudinal profile, cross sections, and slope maps from model run TB1.5, medium K after cession of increased water flux. a)Longitudinal channel profiles show uplift and aggradation, which produces a convexity that propagates upstream. b) Cross sections across the model domain at y=400 show channel aggradation and new lateral erosion of valley walls. c,d,e) Slope maps show valley narrowing following the passage of the knickpoint where y=400 (dashed line) at 155 ky, 159 ky, and 163 ky.

Earth Surf. Dynam. Discuss., doi:10.5194/esurf-2017-28, 2017
Manuscript under review for journal Earth Surf. Dynam.
Discussion started: 8 May 2017

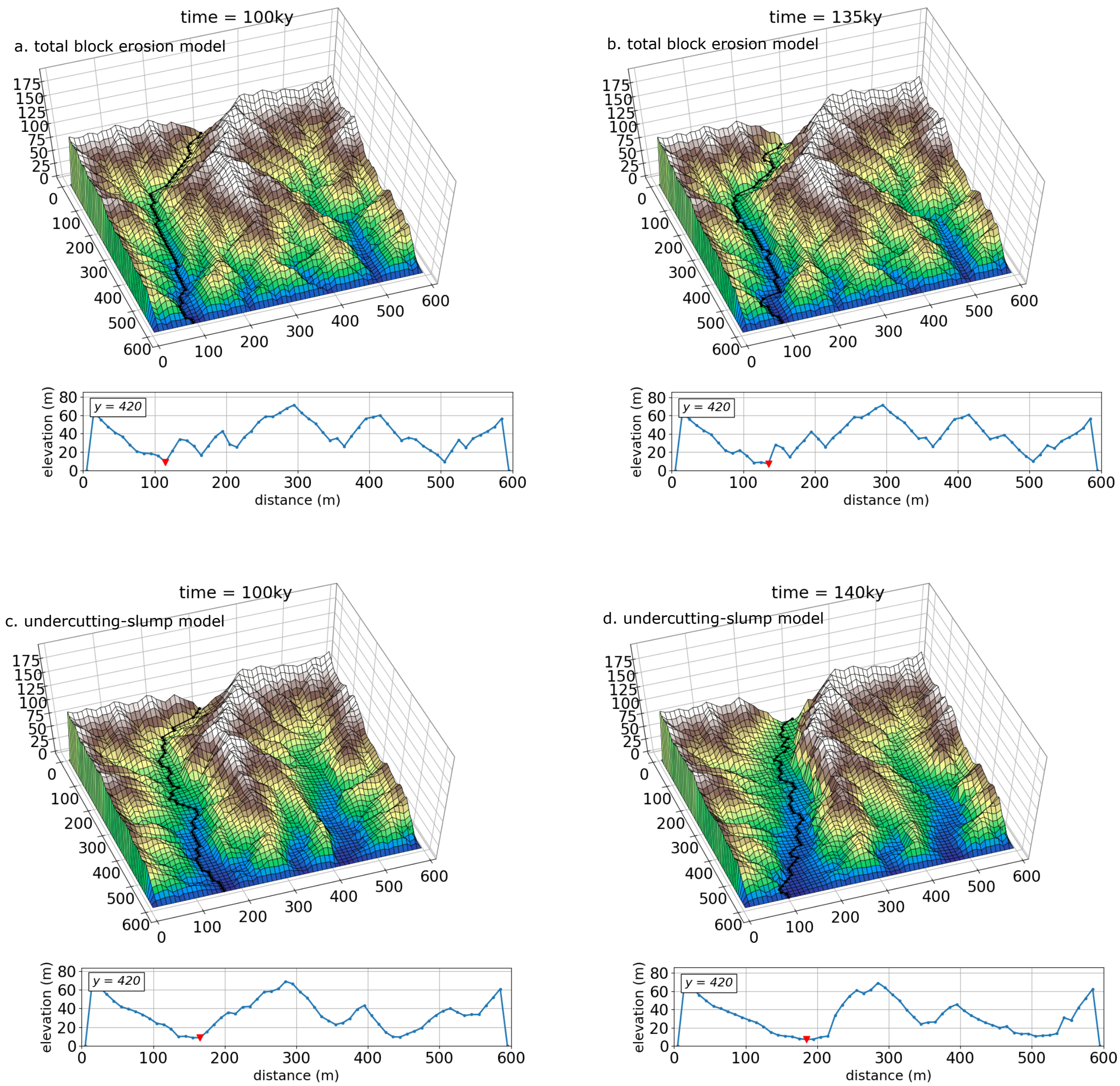

Figure 8. Surface topography and cross section at y=420 during period of increased water flux for the total block erosion models (a,b) and undercutting-slump models (c,d). Red triangle on cross sections indicates the channel position. a) Total block erosion model with low K and $K_l/K_v = 1.0$ at 100 ky, before the increase in water flux. Note that this model looks similar to the spin up model runs with no lateral erosion. b) After 35 ky of increased water flux. Cross section shows incision in the channel and increased relief between the channel and the hillslopes with some valley widening. c) Undercutting-slump model with low K and $K_l/K_v = 1.5$ at 100 ky, before the increase in water flux. Valley is 20 m wide. d) After 40 ky of increased water flux, the channel is slightly lower elevation than before the addition of water flux and the right wall of the valley has eroded by 50 m.

Earth Surf. Dynam. Discuss., doi:10.5194/esurf-2017-28, 2017
Manuscript under review for journal Earth Surf. Dynam.
Discussion started: 8 May 2017

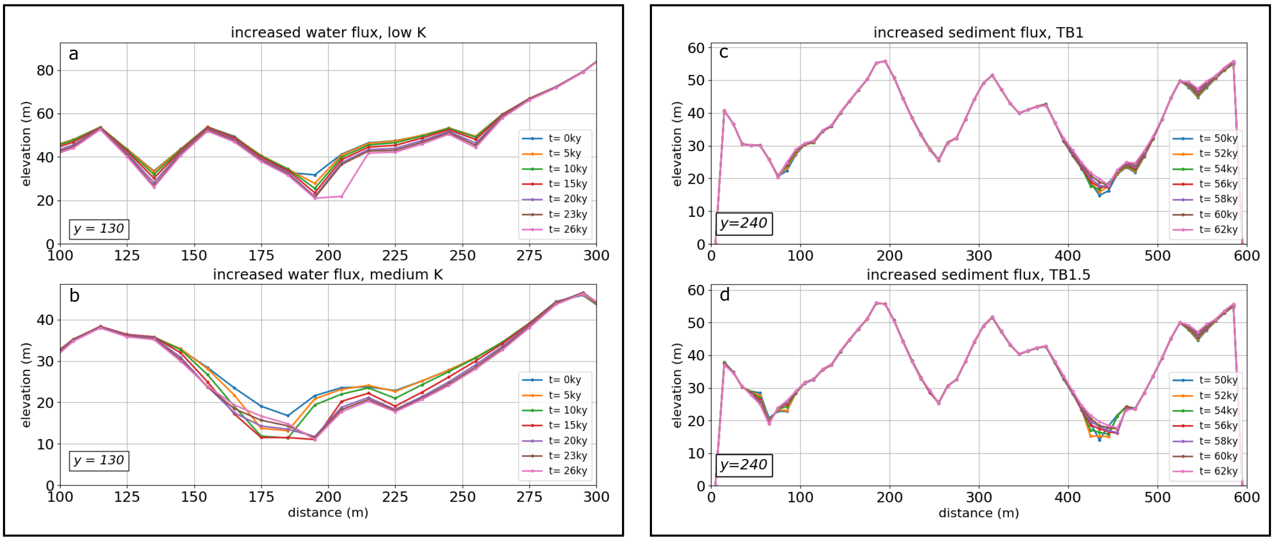

Figure 9. Cross sections across model domain for increased water flux and increased sediment flux models. a,b) Cross section at y=120 for total block erosion models with low erodibility (K=5×10^{-5}) and medium erodibility (K=10^{-4}) during period of increased water flux. Cross sections over 26 ky show vertical incision of channel and increasing relief between the channel and hillslopes initially. After equilibrium is reached, lateral erosion can begin at an increased rate compared to before the additional water flux. c,d) Cross sections at y=240 for total block erosion models with K_l/K_v=1 and $K_l/K_v = 1.5$ during period of increased sediment flux. c) In the TB1 model, the channel aggrades without eroding bedrock walls d)In the TB1.5 model, the channel aggrades and simultaneously erodes bedrock walls.

Earth Surf. Dynam. Discuss., doi:10.5194/esurf-2017-28, 2017
Manuscript under review for journal Earth Surf. Dynam.
Discussion started: 8 May 2017

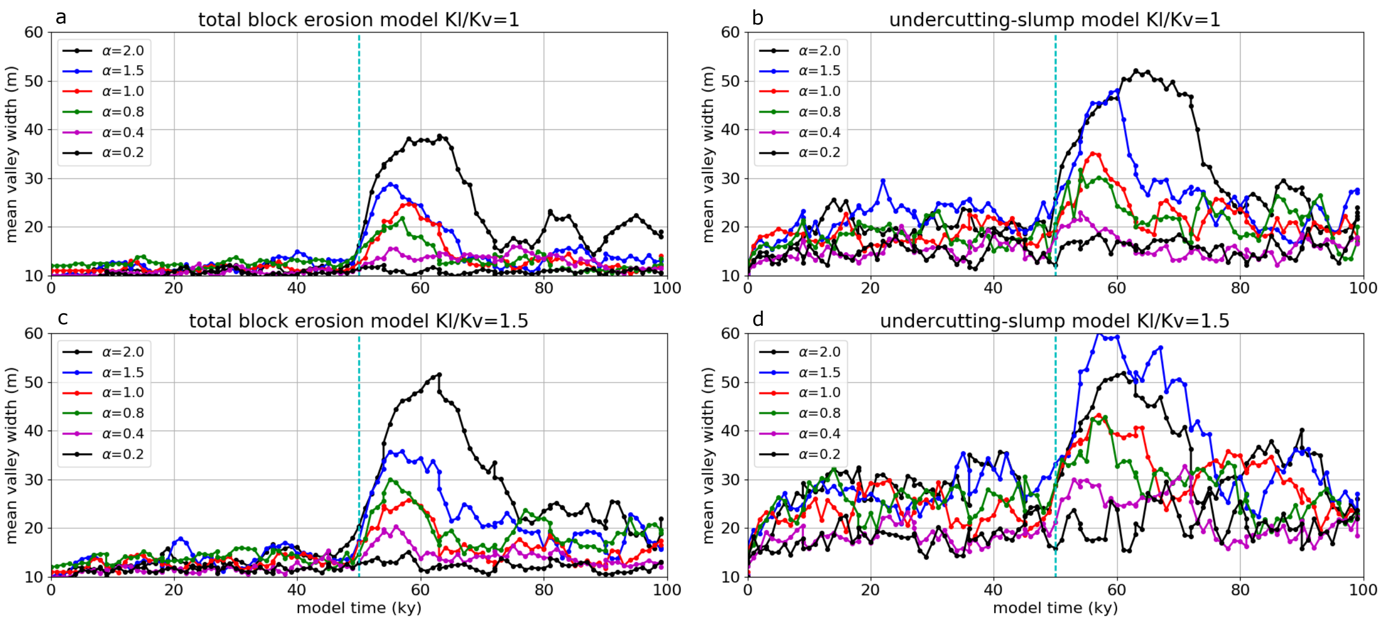

Figure 10. Mean valley width for the upper half of model domain over duration of additional sediment flux model run for total block erosion and undercutting-slump models with K_l/K_v ratio of 1 and 1.5. Dashed light blue line shows when addition of sediment flux began

Earth Surf. Dynam. Discuss., doi:10.5194/esurf-2017-28, 2017
Manuscript under review for journal Earth Surf. Dynam.
Discussion started: 8 May 2017

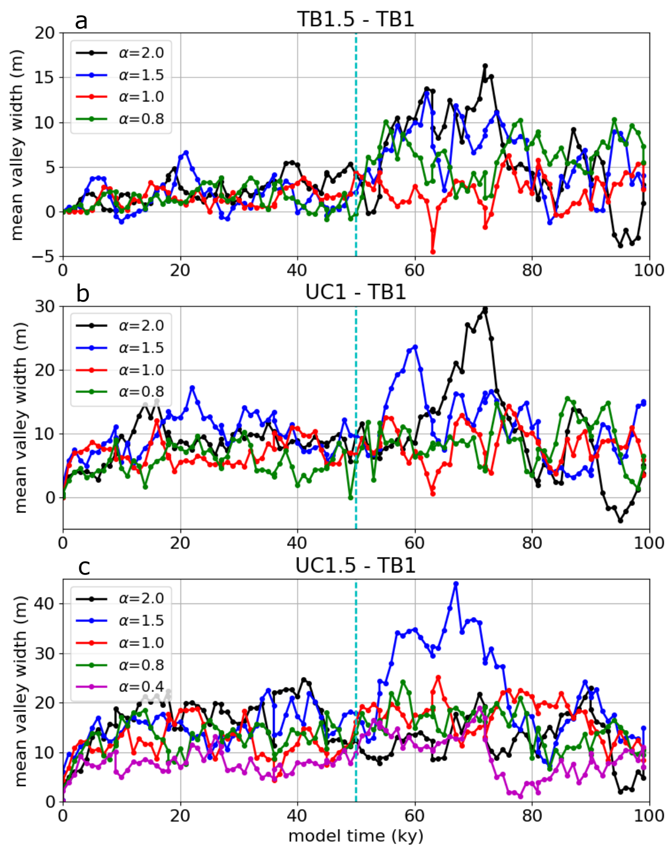

Figure 11. Difference from total block erosion model with $K_l/K_v = 1$ for a)total block erosion model with $K_l/K_v = 1.5$ b) undercutting-slump model with $K_l/K_v = 1$ c) undercutting-slump model with $K_l/K_v = 1.5$. Dashed light blue line shows when addition of sediment flux began

Earth Surf. Dynam. Discuss., doi:10.5194/esurf-2017-28, 2017
Manuscript under review for journal Earth Surf. Dynam.
Discussion started: 8 May 2017

Earth Surface Dynamics
Discussions
Open Access

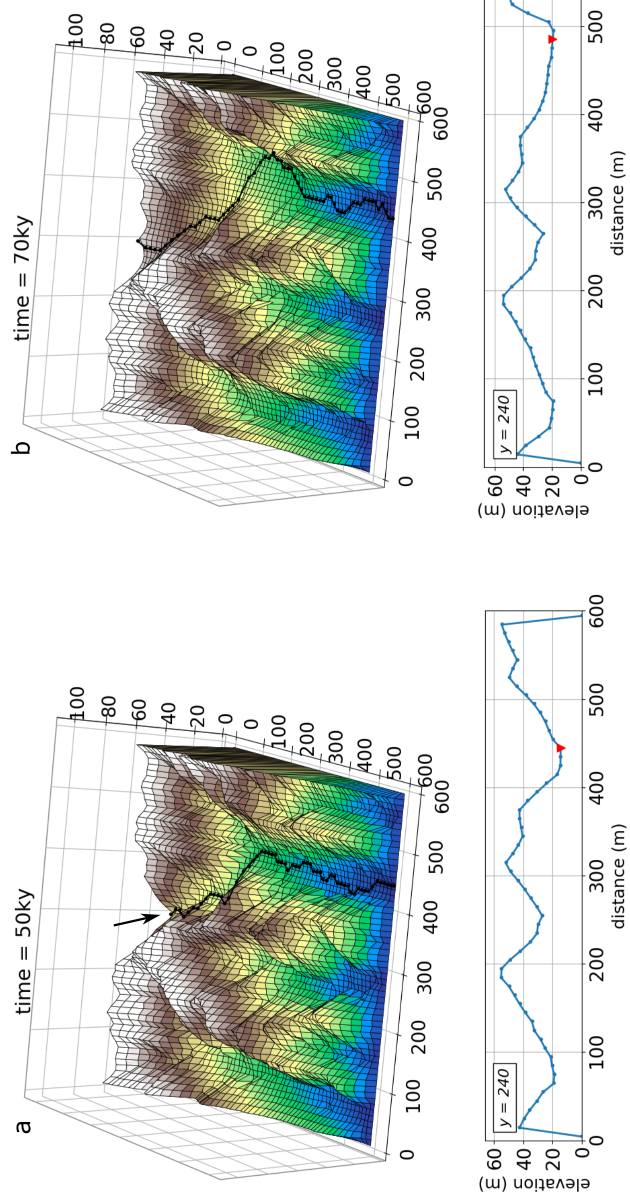

Figure 12. Model topography and cross sections at y=420 during period of increased sediment flux for the undercutting-slump model with α=1.5 and K_l/K_v=1.5. Black line indicates position of the main channel on the landscape. Red triangle shows position of the main channel in the cross section. a) Before increased sediment flux is introduced at input point, indicated with the arrow. b) After 20 ky of increased sediment flux, the channel has aggraded by 5 m and has eroded the valley wall by 50 m.